Carbon sequestration in the subsoil and the time required to stabilize carbon for climate change mitigation

Journal:	*Global Change Biology*
Manuscript ID	Draft
Wiley - Manuscript type:	Review
Date Submitted by the Author:	n/a
Complete List of Authors:	Sierra, Carlos; Max-Plack-Institute for Biogeochemistry, Department of Biological Processes Ahrens, Bernard; Max-Planck-Institut fur Biogeochemie, Biogeochemical Integration Bolinder, Martin Braakhekke, Maarten; VU University Amsterdam von Fromm, Sophie F.; Max-Planck-Institut fur Biogeochemie, Biogeochemical Processes Kätterer, Thomas; Swedish University of Agricultural Sciences, Ecology Luo, Zhongkui; Zhejiang University, College of Environmental and Resources Sciences; Parvin, Nargish; Swedish University of Agricultural Sciences, Soil and Environment Wang, Guocheng; Beijing Normal University, Beijing Normal University, Faculty of Geographical Science
Keywords:	Advection-diffusion-reaction, soil carbon sequestration, Climate change mitigation, transit time, microbial decomposition, organic matter stabilization, radiocarbon
Abstract:	Soils store large quantities of carbon in the subsoil (below 0.2 m depth) that is generally old and believed to be stabilized over centuries to millennia, which suggests that subsoil carbon sequestration can be used as a strategy for climate change mitigation. In this article, we review the main biophysical processes that contribute to carbon storage in subsoil and the main mathematical models used to represent these processes. Our guiding objective is to review whether a process understanding of soil carbon movement in the vertical profile can help us to assess carbon sequestration potential at timescales relevant for climate change mitigation. Bioturbation, liquid phase transport, belowground carbon inputs, mineral association, and microbial activity, are the main processes contributing to the formation of soil carbon profiles, and these processes are represented in models using the advection-diffusion-reaction paradigm. Based on simulation examples, and measurements from carbon and radiocarbon profiles across biomes, we found that advective and diffusive transport may only play a secondary role in the formation of soil carbon profiles. The difference between vertical root inputs and decomposition seems to play a primary role in determining the shape of carbon change

| | with depth. Using the transit time of carbon to assess the timescales of carbon storage of new inputs, we show that only small quantities of new carbon inputs travel through the depth profile and can be stabilized for time horizons longer than 50 years, implying that activities that promote carbon sequestration in the subsoil must take into consideration the very small quantities that can be stabilized in the long term. |
| | |

Carbon sequestration in the subsoil and the time required to stabilize carbon for climate change mitigation

Carlos A. Sierra[1,2], Bernhard Ahrens [1], Martin Bolinder [2], Maarten C. Braakhekke[1],
Sophie von Fromm [1,3], Thomas Kätterer [2], Zhongkui Luo [4], Nargish Parvin [2], and
Guocheng Wang [5]

[1]Max Planck Institute for Biogeochemistry, Germany
[2]Department of Ecology, Swedish University of Agricultural Sciences, Sweden
[3]Department of Environmental Science, ETH Zurich, Switzerland
[4]College of Environmental and Resource Sciences, Zhejiang University, Hangzhou, China
[5]Beijing Normal University, Beijing, China

June 2, 2023

1 **Abstract**

2   Soils store large quantities of carbon in the subsoil (below 0.2 m depth) that is generally old and
3   believed to be stabilized over centuries to millennia, which suggests that subsoil carbon seques-
4   tration can be used as a strategy for climate change mitigation. In this article, we review the
5   main biophysical processes that contribute to carbon storage in subsoil and the main mathematical
6   models used to represent these processes. Our guiding objective is to review whether a process
7   understanding of soil carbon movement in the vertical profile can help us to assess carbon seques-
8   tration potential at timescales relevant for climate change mitigation. Bioturbation, liquid phase
9   transport, belowground carbon inputs, mineral association, and microbial activity, are the main
10 processes contributing to the formation of soil carbon profiles, and these processes are represented
11 in models using the advection-diffusion-reaction paradigm. Based on simulation examples, and
12 measurements from carbon and radiocarbon profiles across biomes, we found that advective and
13 diffusive transport may only play a secondary role in the formation of soil carbon profiles. The dif-
14 ference between vertical root inputs and decomposition seems to play a primary role in determining
15 the shape of carbon change with depth. Using the transit time of carbon to assess the timescales
16 of carbon storage of new inputs, we show that only small quantities of new carbon inputs travel
17 through the depth profile and can be stabilized for time horizons longer than 50 years, implying
18 that activities that promote carbon sequestration in the subsoil must take into consideration the
19 very small quantities that can be stabilized in the long term.

20 **Keywords**: Climate change mitigation, soil carbon sequestration, transit time, advection-diffusion-
21 reaction, microbial decomposition, organic matter stabilization, radiocarbon

Contents

1 Introduction

Soil carbon stocks below surface horizons (below 0.2 m depth) are not only one of the largest carbon (C) reservoir of the terrestrial surface, but are also relatively old as demonstrated by radiocarbon measurements (Mathieu et al., 2015; He et al., 2016; Shi et al., 2020; Heckman et al., 2022). These radiocarbon measurements along the vertical profile have shown that the age of carbon increases significantly with depth, indicating that carbon may be stabilized for centuries to millennia in the subsoil. It is therefore reasonable to think that soils could act as a large sink for fossil-fuel derived carbon if subsoil carbon sequestration is promoted, particularly in agricultural and managed lands (Button et al., 2022).

The subsoil has a large influence on ecosystem productivity and the supply of ecosystem services. It has been estimated that between 10 and 80% of the nutrient and water requirement of plants are provided by the subsoil (Hinzmann et al., 2021). Carbon sequestered in subsoils generally contributes to more than half of the total stocks within a soil profile. However, the amount of organic C stored in soil varies among biomes; relative to the first meter, between 43 and 71% of soil organic carbon (SOC) is found at depths below 20 cm (Jobbágy and Jackson, 2000). In agricultural soils, the amount of soil organic carbon stored in subsoils (up to 1 m depth) is similar to that in the topsoil arable layer (Morari et al., 2019). Studies in agroecosystems often consider only the arable layer (> 90 % observations), where most changes in soil C are assumed to occur because C cycling is more dynamic in topsoil compared to deeper soil layers (Bolinder et al., 2020). However, this does not imply that subsoil C is insensitive to agricultural management practices. There is evidence from long-term field experiments that management practices affect C stocks at decadal timescales in the upper part of the subsoil or even deeper (e.g. Kirchmann et al., 2013; Kätterer et al., 2014; Menichetti et al., 2015; Börjesson et al., 2018; Dal Ferro et al., 2020; Slessarev et al., 2020).

Furthermore, effects on subsoil carbon are evident when comparing annual versus perennial crops with more well developed root systems or versus other deep rooting species (Carter and Gregorich, 2010; Collins et al., 2010; VandenBygaart et al., 2011; Guan et al., 2016). Major land-use changes such as cropland to grassland, or cropland to forest and vice versa, may also in some cases induce changes in subsoil carbon (Guo and Gifford, 2002; Poeplau and Don, 2013). Button et al. (2022) reviewed several other options than the traditional management practices for increasing subsoil C, such as burial of organic matter or biochar addition to the subsoil. There is a need for including subsoil carbon in model-based estimates of carbon sequestration (Button et al., 2022), but the mechanisms governing the effect of changes in subsoil carbon are understudied, which has been identified as a major knowledge gap (Lorenz and Lal, 2005; Chenu et al., 2019) while raising awareness of the potential for subsoils to promote SOC sequestration (Kautz et al., 2013; Chen et al., 2018).

Indeed, the use of deep-rooting plant species has been suggested as a land management strategy to promote carbon input to subsoil and thus sequestering soil carbon and mitigating climate change in cropping systems (Kell, 2011; Thorup-Kristensen et al., 2020). However, there is conflicting information regarding the time new carbon inputs to subsoil would be stabilized on decadal timescales. Recent quantifications of the transit time of carbon inputs across soil depth showed that carbon inputs transit fast in all soil layer depths, challenging the efficiency of promoting carbon inputs to subsoil for soil carbon sequestration (Xiao et al., 2022; Wang et al., 2023).

Managing soils for C sequestration purposes implies that the fate and transit time of new carbon inputs can be acurately quantified (Crow and Sierra, 2022). Mathematical models of subsoil carbon dynamics play an important role for this purpose, and can be used to estimate the potential for subsoil carbon sequestration due to land management.

In this review, we survey the main processes that contribute to soil carbon storage and dynamics in the subsoil, with particular emphasis on mathematical models of subsoil carbon dynamics. We focus on most natural processes, but we do not consider the vertical redistribution of C along the profile through tillage or other human interferences, which can cause a sudden change in SOC distribution that may have impact on C dynamics. Our guiding question is whether a process understanding of soil C movement through the vertical profile can help us to assess C sequestration potential at timescales relevant for climate change mitigation. For this purpose, we first review process understanding of subsoil C dynamics, and then review mathematical models used in the past to represent these processes.

Based on this review, we show that most previous models can be generalized under one single modeling paradigm, and through examples, show the main contribution of different processes in shaping soil carbon profiles. In addition, we present a conceptual framework to assess the fate of new carbon inputs as they move through the subsoil. We use the theoretical framework provided by the transit time distribution of carbon in compartmental systems (Sierra et al., 2017, 2018b; Metzler and Sierra, 2018), and discuss our results in the context of soil carbon management for climate change mitigation.

2 Processes contributing to the formation of soil carbon profiles

The accumulation of organic carbon in the vertical profile is an important part of soil formation (Jenny, 1980; van Breemen and Buurman, 1997), taking place on timescales of decades to millennia. Overall, soil carbon dynamics is determined by the gain and loss (above and belowground) of carbon inputs, and decomposition. When studying the vertical distribution of soil carbon, the depth dependence of these processes is relevant, as well as vertical transport, erosion and deposition. Vertical organic matter transport can have a major effect on the soil carbon profile and is generally caused by mixing processes and transport of mobile fractions with the liquid phase (van Breemen and Buurman, 1997; Rumpel and Kögel-Knabner, 2011). In terrestrial soils, mixing of the soil—referred to as "pedoturbation" (Hole, 1961)—can occur by several processes, including the reworking activity of soil fauna (bioturbation), freezing and thawing (cryoturbation) (Johnson et al., 1987) and human disturbance such as tillage. Cryoturbation occurs mainly in permafrost affected soils, which cover large regions at high latitudes. In other systems however, bioturbation and liquid phase transport are the main transport processes that redistribute carbon vertically.

In layers with high organic matter concentrations, an important additional transport flux occurs that is generally ignored in soil carbon profile models. Loss of mass due to decomposition leads to downward shift of material above, while surface litter deposition continually buries older material. This mass-loss causes advective downward or upward flow of material unrelated to mixing or water movement (Ahrens et al., 2015). (Kaste et al., 2007) found this process to be relevant for the vertical distribution of 210Pbex in the organic surface horizon of a podzol, and Hilbert et al. (2000) for modelling subsidence of peat soils.

2.1 Bioturbation

Bioturbation is defined as the biological reworking of soils and sediments by different kinds of organisms, including plant rooting systems, and most importantly, burrowing animals (Meysman et al., 2006). Chapin et al. (2002) noted that in temperate regions the mixing activity of earthworms represents a force that is orders of magnitude larger than other geomorphic processes such as erosion. The potential effects of bioturbators on their habitat are so severe that they have been called "ecosystem engineers" (Meysman et al., 2006). The rate of soil displacement by bioturbating organisms is usually estimated by measuring deposition of mounds at the soil surface. Paton et al. (1995) reviewed a range of quantitative estimates for different organisms. They concluded that the most important animal groups are earthworms, ants, mammals, and termites, with rates of mounding that can range from 0.0063 to 27 kg m^{-2} yr^{-1} .

Soil mixing by bioturbation has a homogenizing effect on soil properties: it increases dispersal of particles, reduces concentration gradients, and destroys layering (Johnson et al., 1987). Hence, bioturbation leads to organic matter diffusion and potentially to deepening of the soil profile. However, at small spatial scales the effects of bioturbation are more complex, for several reasons: (i) Certain fractions may be transported preferentially. For example, since mixing by earthworms is mostly related to feeding, it is more likely to affect (fresh) litter rather than mineral fractions (Johnson et al., 2005). The coarsest fractions, including stones, may be completely unaffected by bioturbation. (ii) Mixing may occur more strongly in one direction than in others (anisotropic mixing). For example termites bring clay particles from considerable depths to the soil surface for incorporation into their surface mounds (Paton et al., 1995). (iii) The distance of particle translocation may be in some cases quite large compared to the scale of a single soil profile (Boudreau, 1986a).

Although the relevance of bioturbation for organic matter redistribution is well recognized (van Breemen and Buurman, 1997; Chapin et al., 2002; Hoosbeek and Scarascia-Mugnozza, 2009), very few empirical studies have been performed on its effects on the shape of the soil C profile (Tonneijck and Jongmans, 2008; Yoo et al., 2011), particularly on long timescales. Based on micromorphological analysis and radiocarbon measurements, Tonneijck and Jongmans (2008) showed that bioturbation was the main mechanism for carbon input at depth in a volcanic ash soil, more important than liquid phase transport and root input. On shorter time scales, studies of earthworm invasions in forests have demonstrated dramatic effects on organic surface layers (Alban and Berry, 1994; Bohlen et al., 2004). For example, Alban and Berry (1994) found that increasing earthworm populations in a temperate podzol led to a reduction of forest floor mass by 85 % and disappearance of the eluviation horizon in 14 years.

2.2 Liquid phase transport

A small part of organic matter in soils is dissolved in the liquid phase. Concentrations of dissolved organic carbon (DOC) are typically so low that total organic carbon in solution is negligible compared to the immobile fraction (Michalzik et al., 2001). However, leaching and decomposition fluxes of dissolved organic matter may be important terms in shaping the dynamics of soil carbon at depth (Kalbitz and Kaiser, 2008; Kindler et al., 2011; Kaiser and Kalbitz, 2012). DOC is highly relevant for the formation of the soil profile since it is subject to potentially very fast transport with downward water fluxes and represents a mechanism of organic matter input at depths well below the zone where bioturbation and root input are relevant (Rumpel et al., 2012). Furthermore, adsorption of DOC to the mineral phase is one of the main mechanisms for organic carbon stabilization and persistence (Kalbitz and Kaiser, 2008). DOC is not chemically well defined, but consists of a broad spectrum of organic substances ranging from small molecules to complex humic acids (Kalbitz et al., 2000; Michalzik et al., 2001). The biodegradability of these substances ranges over several orders of magnitude (Kalbitz et al., 2000), with more resistant compounds generally increasing with depth (Kalbitz et al., 2000; Sanderman et al., 2008).

DOC may originate from several sources, with their relative contribution being highly variable for different ecosystems (Kalbitz et al., 2000; Chantigny, 2003). Leaching of fresh litter contributes strongly to DOC production in the surface organic layer. However, for most plant species litter leachate is relatively labile, and thus may not contribute strongly to DOC in the mineral soil (Neff and Asner, 2001). More complex and recalcitrant dissolved organic substances may be formed predominantly as a byproduct of decomposition, contributing more to DOC in the mineral soil.

DOC also enters the soil by throughfall (Michalzik et al., 2001), and root exudation (Neff and Asner, 2001), and it is removed from the soil solution by uptake and decomposition by microbes. A considerable part of DOC is easily degradable, with low molecular weigh compounds decreasing strongly with depth (Roth et al., 2019). Another important mechanism for DOC removal is immobilization due to interactions with the solid phase and (co-)precipitation. Through a range of chemical mechanisms, DOC is adsorbed to surfaces of minerals (particularly Al and Fe hydroxides and clay) and to a lesser extent to solid organic matter (Neff and Asner, 2001). These interactions are highly variable and depend on the chemical properties of DOC, the sorbent, and the soil solution. Furthermore, in acid soils DOC may (co-)precipitate with Al and Fe ions, which is an important process for the formation of the illuviation horizon in podzols (van Breemen and Buurman, 1997). As a result of these interactions, the apparent vertical transport of DOC is significantly lower than that of water, and DOC concentrations are often much lower in the deep soil than near the surface.

2.3 Depth dependence of organic matter input

Total litter input to soil can be divided into an aboveground fraction: leaves/needles, stems, branches, and fruits; and a belowground fraction, also referred to as rhizodeposition: root mortality, sloughing off of root tissue, and secretion of mucilage and root exudates (Nguyen, 2009). The relative distribution of the litter input over these two fractions, as well as the vertical distribution of the belowground input is highly relevant for the carbon profile. Jobbágy and Jackson (2000) found a significant relationship

between vertical soil carbon distribution and plant functional type, which is partially explained by ecosystem-level root/shoot ratios and the vertical distribution of root biomass. Since net primary production (NPP) is the source of litter input, its distribution over above- and below-ground biomass is a good predictor of the relative proportions of aboveground litter fall and rhizodeposition (Raich and Nadelhoffer, 1989; Xiao et al., 2023). For instance, herbaceous vegetation types and shrubs allocate the highest fraction of NPP belowground, and forests the lowest fraction (Chapin et al., 2002). Saugier et al. (2001) compiled NPP estimates and concluded that on average 67 % and 57 % of NPP is allocated belowground for grasslands and arctic tundra, respectively, whereas for temperate and boreal forests this fraction is 39 % and 44 %. The proportion for common annual agricultural crops and perennial forages represents about 20 % and 50 %, respectively (Bolinder et al., 2007). Root to shoot biomass ratios follow a similar pattern (Jackson et al., 1996). Due to the difficulty of measuring NPP, particularly belowground, these figures should be considered carefully (Clark et al., 2001). Synthesizing global data sets including NPP measurements from 725 soil profiles, root biomass and its depth distribution from 559 soil profiles, Xiao et al. (2023) recently mapped depth-resolved belowground NPP (BNPP) at 1 km resolution across the globe. They found that global average BNPP allocated to the 0–20 cm soil layer is estimated to be 1.1 Mg C ha^{-1} yr^{-1}, accounting for $\sim$60% of total BNPP. Across the globe, the depth distribution of BNPP varies largely, and more BNPP is allocated to deeper layers in hotter and drier regions. Edaphic, climatic and topographic properties (in order of importance) explain $>$ 80% of such variability; and the direction and magnitude of the influence of individual properties are soil depth- and biome-dependent (Xiao et al., 2023). Furthermore, plants may change their allocation pattern and rooting profile when changes in nutrient and water availability and other environmental factors occur (Jackson et al., 2000).

Decomposition dynamics of above and belowground litter differ substantially due to differences in chemical composition and environmental factors at the deposition site—at the surface or directly within the profile. Root litter has repeatedly been found to be more chemically recalcitrant than aboveground litter due to the presence of substances such as lignin, cutin, and suberin (Rasse et al., 2005). Furthermore, since root input occurs predominantly in the mineral soil, it is subject to stabilization mechanisms related to the mineral phase such as adsorption and occlusion in aggregates (Rasse et al., 2005).

Rhizodeposition is vertically distributed over the mineral soil profile and organic surface layers. Jackson et al. (2000) analysed a global data set of root distribution measurements and found that tundra, boreal forests and temperate grasslands generally have the shallowest profiles with 80–90 % of the roots occurring at the top 30 cm of the soil. Deserts and temperate coniferous forests had the deepest rooting profiles with only 50 % of the roots in the top 30 cm. In a review for temperate agricultural crops, Fan et al. (2016) showed that 50% of the roots were accumulating in the upper 8 – 20 cm. Independent of vegetation type, root distribution seems to be mostly determined by soil hydrology, as demonstrated by significant relationships between annual potential evapotranspiration, precipitation, and soil texture (Schenk and Jackson, 2002a). In more water limited ecosystems, plants tend to have deeper root profiles to maximize water uptake (Schenk and Jackson, 2002b). Roots may also preferentially grow in the organic surface layer, if present, due to the high nutrient and moisture availability there (Jordan and Escalante, 1980; Schenk and Jackson, 2002a). Although rhizodeposition and root biomass are strongly related, they may not have exactly the same vertical distribution, since not all roots contribute equally to rhizodeposition. Fine roots have higher mortality rates and excrete more exudates since they play a greater role in water and nutrient uptake (Anderson et al., 2003). Hence, it is likely that organic matter input by roots is more closely related to the fine root profile, which is more shallow than the overall distribution of roots. Furthermore, radiocarbon analysis shows that also within the fine root fraction, production and mortality rates decrease with depth (Gaudinski et al., 2010). In a study with pulse-labelled ^{13}C-CO$_2$, Hirte et al. (2018) found that the proportion of rhizodeposition C of belowground inputs increased with soil depth for maize and wheat. Thus, rhizodeposition remains to be one of the most difficult C input sources to quantify, with a wide range of estimates that also depends on plant species/cultivars and growth stages (e.g. Amos and Walters, 2006; Pausch and Kuzyakov, 2018).

2.4 Depth dependence of soil organic matter properties and dynamics

The chemical properties of soils change along the vertical profile (Rumpel and Kögel-Knabner, 2011; Vancampenhout et al., 2012). Most well-known are the decrease of C/N ratio with depth, and the enrichment of ^{13}C and ^{15}N (Ehleringer et al., 2000; Nadelhoffer and Fry, 1988; Högberg, 1997; Paul et al., 2020). These gradients indicate a change from plant derived to more decomposed and microbial derived organic matter with depth (Rumpel et al., 2002; Rumpel and Kögel-Knabner, 2011; Baisden et al., 2002). It has been suggested that microbial residues are more effectively stabilized by organo-mineral interactions, which have been found to be an important mechanism in the deep soil (Rumpel et al., 2012).

A distinct property of most soils is the decrease of radiocarbon (^{14}C) activity with depth, indicating a higher average age of carbon since plant uptake from the atmosphere. Near the surface, average radiocarbon age is typically in the range of 1 to 100 yr, whereas in the deep soil ages of 10 000 yr or more are no exception (Mathieu et al., 2015; He et al., 2016; Lawrence et al., 2020; Rumpel and Kögel-Knabner, 2011). Presumably, this age gradient is partially explained by slow downward transport of carbon fractions that are either very recalcitrant, or recurrently recycled by microbes (Elzein and Balesdent, 1995; Kaiser and Kalbitz, 2012). However, a more important cause may be decreasing average decomposition rates along the profile (Jenkinson and Coleman, 2008; Koven et al., 2013; Persson et al., 2000). The reason for this gradient is not fully understood yet and needs further exploration (Guo et al., 2023). It may be caused by the selective preservation of recalcitrant compounds combined with downward transport (Elzein and Balesdent, 1995; Luo et al., 2020) or nonlinear interactions among C fractions (Guenet et al., 2013; Liang et al., 2018). Also, the dominant source of organic matter in deep soils is root input, which is chemically more recalcitrant than aboveground litter (Rasse et al., 2005).

Another cause of the decreasing decomposition rates with depth is the increased occurrence of certain stabilization mechanisms. Several studies have found that organic matter in subsoils is predominantly associated with minerals (Rumpel and Kögel-Knabner, 2011; Eusterhues et al., 2003) (Rasmussen et al., 2018) or occluded within aggregates (Moni et al., 2010). A further cause of stabilization in deep soil is physical disconnection between microbes and substrates (Don et al., 2013). Most microbial activity in deep soils is located in so-called hot spots: root and earthworm channels and preferential water flow paths (e.g. cracks). Organic matter outside of these zones may be stabilized due to spatial separation from decomposers (Chabbi et al., 2009).

3 Soil carbon profile models

While the overwhelming majority of soil carbon models do not represent spatial processes (Manzoni and Porporato, 2009), a small number of models have been published that in some way account for the vertical soil carbon profile. For example, some models vertically distribute simulated total soil organic carbon or extrapolate topsoil carbon downwards using a predefined depth-function, in order to determine lateral soil carbon transport due to erosion (Rosenbloom et al., 2001; Hilinski, 2001). Several models represent carbon pools in predefined soil layers that differ with respect to physical and chemical parameters, as well as temperature, moisture, and root input (van Veen and Paul, 1981; Grant et al., 1993). In some cases heat or water transport between layers is included to account for the effects of temperature and moisture on decomposition, or to simulate leaching of mineral nitrogen (Hansen et al., 1991; Li et al., 1992). However, these models do not consider explicitly vertical transfer of organic matter between layers. A number of models of DOC dynamics have been proposed (Michalzik et al., 2003; Neff and Asner, 2001; Gjettermann et al., 2008; Brovelli et al., 2012). These models account explicitly for production and mineralization of DOC, as well as vertical transport with water flow and ad- and desorption. Transport is usually represented as advection, based on measured or simulated water fluxes. These schemes are mainly developed to reproduce DOC fluxes and concentrations at small scales, and usually require site level calibration or detailed information on soil texture.

The effects of bioturbation in terrestrial soils have been modeled in relation to transport of radionuclides (e.g. Müller-Lemans and van Dorp, 1996; Kaste et al., 2007; Bunzl, 2002) and soil formation (Kirkby, 1977; Salvador-Blanes et al., 2007). More literature exists on modelling of benthic bioturba-

7

299 tion and its effects on chemical species in sediments at the bottom of oceans and lakes (e.g. Boudreau,
300 1986a; Meysman et al., 2005, 2010; Sarmiento and Gruber, 2006; Arndt et al., 2013). Bioturbation is
301 usually modeled as a diffusive process, although it has been shown that this approach is not generally
302 valid (Meysman et al., 2003, 2010). Alternatively, other schemes have been proposed to represent dif-
303 fusive processes, which includes both deterministic (Boudreau, 1986b, 1989) and stochastic approaches
304 (Bunzl, 2002; Choi et al., 2002; Meysman et al., 2008).

305   Perhaps the first model truly aimed at dynamically simulating the soil carbon profile was developed
306 by Kirkby (1977), as part of a soil formation model. Since then, a number of models have been
307 developed that combine decomposition with vertical transport, represented either as diffusion (O'Brien
308 and Stout, 1978; van Dam et al., 1997; Koven et al., 2009), advection (Nakane and Shinozaki, 1978;
309 Dörr and Münnich, 1989; Bosatta and Ågren, 1996; Feng et al., 1999; Baisden et al., 2002; Jenkinson
310 and Coleman, 2008), or both (Elzein and Balesdent, 1995; Bruun et al., 2007; Freier et al., 2010;
311 Guenet et al., 2013; Koven et al., 2013; Braakhekke et al., 2011, 2013). Most of these models were
312 developed to explain measurements of carbon and tracer profiles. Increasingly, more models are now
313 developed to represent soil carbon cycling and predict land-atmosphere carbon exchange (Jenkinson
314 and Coleman, 2008; Huang et al., 2018; Koven et al., 2013; Ahrens et al., 2020; Luo et al., 2020).

3.1   A general model of soil carbon transport and decomposition with depth

316 The main processes involved in the formation of soil carbon profiles, bioturbation, liquid phase trans-
317 port, rhizodeposition, and decomposition, are commonly represented in models using the mathematical
318 paradigms of diffusion, advection, and reaction, respectively. It is therefore useful to conceptualize
319 models of SOM transport and dynamics by a general paradigm expressed as

$$\frac{\partial x(d,t)}{\partial t} = \text{Diffusion} + \text{Advection} + \text{Reaction}, \tag{1}$$

320 where the variable x represents soil organic matter or carbon, and variable t represents time. We use
321 here partial derivatives (the ∂ symbol) to represent the change of soil carbon with respect to time,
322 assuming that it can also change along a variable d that denotes soil depth. Therefore, we are also
323 interested in representing changes in x with depth; i.e. $\partial x/\partial d$. Equation 1 is a continuity equation,
324 expressing how the conserved quantity x, which obeys mass conservation, changes continually with
325 soil depth and time.

326   Our main postulate is that all models of vertical SOC transport are special cases of 1, expressing
327 different forms of diffusion, advection and reaction. This general approach to modeling vertical dy-
328 namics has been identified previously for diverse systems such as marine organic matter (Sarmiento
329 and Gruber, 2006) or sediments (Arndt et al., 2013).

3.1.1   Diffusion

331 Processes related to bioturbation are commonly represented in models using diffusion equations. A
332 simple general model of soil carbon profile dynamics including only vertical diffusion and inputs can
333 be expressed as

$$\frac{\partial x(d,t)}{\partial t} = \frac{\partial}{\partial d}\left(\kappa(d,t)\frac{\partial x(d,t)}{\partial d}\right) + u(d,t), \tag{2}$$

334 where $\kappa(d,t)$ is a function that represents how mass diffusivity depends on soil depth and time. Mass
335 diffusivity is a soil property that generally does not change considerably over short timescales. Some
336 models represent changes in diffusion with depth as a function of bulk density. In the most simple
337 case it can be expressed as a constant κ with no depth dependence. The function $u(d,t)$ expresses
338 how litter and root inputs change with depth and time, and can take multiple forms depending on
339 attributes of the vegetation such as phenology, allocation, and rhizodeposition.

340   Models of the form of equation 2 can only be solved (analytically or numerically) if initial conditions
341 $x(d,0)$ are known as well as the carbon contents or their change at two points along the vertical profile,
342 between a depth at the surface d_0 and some maximum depth $d_{\max}$. The latter are called the boundary
343 conditions, and must be known a priori in order to obtain solutions of these models.

To obtain an intuitive understanding of potential solutions to this model, it is useful to assume mass diffusivity as a constant (κ) and that inputs of organic matter to the soil are constant over time according to some function $u(d)$ where the inputs change with depth. Under these conditions, the soil carbon content along the profile reaches a steady-state in which it does not change over time; i.e.,

$$\frac{\partial x(d,t)}{\partial t} = 0,$$

and the steady-state carbon content along the profile $x(d)$ is the solution to the second order ordinary-differential equation

$$\frac{\partial^2 x}{\partial d^2} = -\frac{u(d)}{\kappa}. \tag{3}$$

Again, this equation can be solved using boundary conditions, integrating with respect to d to obtain the distribution of carbon content with depth $x(d)$. Equation 3 implies that the steady-state carbon content in a diffusion controlled environment is mostly defined by the relation between the depth distribution of inputs and the mass diffusivity of the soil. The vertical distribution of inputs is mostly a property of the vegetation and the rhizosphere system, while mass diffusivity is mostly a property of the soil and the organisms that act as bio-engineers.

3.1.2 Advection

The other main mathematical paradigm used to represent vertical processes in soil carbon profiles is advection; i.e., the transport of organic carbon dissolved in water. Following mass conservation, advection can be expressed as

$$\frac{\partial x(d,t)}{\partial t} = -\frac{\partial}{\partial d}f(x(d,t)), \tag{4}$$

where $f(x(d,t))$ is the flux or flow rate of mass at depth d and time t. In other words, the mass of soil carbon can only change over time due to the flow rate of the fluid along a vertical direction. If the fluid is flowing at a constant velocity v, equation 4 can be simplified to

$$\frac{\partial x(d,t)}{\partial t} = -v\frac{\partial x(d,t)}{\partial d}. \tag{5}$$

Intuitively, this implies that soil carbon is removed from a depth d at the velocity at which the fluid is passing through, and the gradient at which carbon content changes with depth. Flow velocity is determined by the combination of all the physical, chemical, and biological factors that affect water flow in saturated and unsaturated soils. Although flow velocity may not be constant in most cases, equation 5 helps to understand its role in modeling SOM transport mechanisms in soils.

To better understand the role of $f(x(d,t))$ in equation 4, it is useful to think of $x(d,t)$ as a density function (LeVeque, 1990) that represents the mass concentration of SOM at a particular depth and time. Therefore, the total mass of carbon between two depths d_1 and d_2 at time t is given by

$$\int_{d_1}^{d_2} x(d,t)\ \mathrm{d}d.$$

Because in an advection only system the total mass between the depths d_1 and d_2 only changes due to the flux at the end points, we can assume that

$$\frac{\mathrm{d}}{\mathrm{d}t}\int_{d_1}^{d_2} x(d,t)\mathrm{d}d = f(x(d_1,t)) - f(x(d_2,t)). \tag{6}$$

The function $x(d,t)$ is not know explicitly, therefore we do not have explicit formulas for the flow rates f. Nevertheless, equation 6 helps to understand the role of the flow rate function f in equation 4; it represents the flow rate of soil carbon at any given depth and time.

3.1.3 Reaction (decomposition)

If we ignore vertical transport, soil carbon would display temporal dynamics related to the action of microorganisms and how they consume organic matter. This process of decomposition has been studied extensively, and there are hundreds of mathematical models that represent these dynamics ignoring vertical transport processes (Manzoni and Porporato, 2009). Despite the large variety of models, most of these models can be expressed in a general expression of the form (Sierra and Müller, 2015; Sierra et al., 2018a)

$$\frac{\mathrm{d}\boldsymbol{x}}{\mathrm{d}t} = \boldsymbol{u}(\boldsymbol{x}, t) + \mathbf{B}(\boldsymbol{x}, t) \cdot \boldsymbol{x}(t). \tag{7}$$

This general model is expressed in vector (lower case bold) and matrix (upper case bold) form because it is assumed that soil organic carbon is highly heterogeneous, and different proportions decompose at different rates. Therefore, the vector $\boldsymbol{x}(t) \in \mathbb{R}^n$ represents the mass of soil carbon in n number of compartments at time t. The total mass at time t, $x(t)$, can be simply obtained as the sum of the elements of this vector, i.e. $x(t) = \|\boldsymbol{x}(t)\|$ (the vertical bars indicate a sum of the positive elements of a vector). Mass inputs to this system are represented by the vector $\boldsymbol{u}(\boldsymbol{x}, t)$, which expresses the amount of organic matter inputs that would enter each compartment. Because above and belowground litter inputs can differ in their chemical and physical properties, different proportions of the total mass may enter different compartments. In addition, the inputs may depend on the amount of carbon in particular compartments; for example, if exudation rates depend on the amount of mycorrhiza. For this reason, the inputs $\boldsymbol{u}$ are expressed as dependent on the amount of mass present in the compartments at any given time.

Rates of decomposition and transfer of carbon among compartments are expressed in the matrix $\mathbf{B}(\boldsymbol{x}, t)$ of equation 7. This matrix is called compartmental because it has important mathematical properties related to mass conservation: all diagonal elements are non-positive, all off-diagonal elements are non-negative, and the column sums are non-positive (Metzler and Sierra, 2018; Sierra et al., 2018a).

Linear models such as Century and RothC as well as nonlinear microbial models such as those proposed by soil ecologists (e.g Schimel and Weintraub, 2003; Allison et al., 2010) are especial cases of the general model of equation 7 (Sierra and Müller, 2015), whose internal structure helps to study particular aspects of decomposition processes that are independent of vertical transport. These processes include: differences in the decomposability of different types of organic matter, organo-mineral interactions, effects of abiotic variables such as temperature, moisture, and pH on the rates of organic matter processing, interactions between substrates and microbial groups, among others.

To incorporate vertical transport processes in this model, we can assume that at any given depth d, reaction (decomposition) processes are expressed as

$$\frac{\partial x(d, t)}{\partial t} = \left\| \frac{\mathrm{d}\boldsymbol{x}(d, t)}{\mathrm{d}t} \right\| \tag{8}$$

where the sum is over all the compartment contents at any given depth and time. Notice that this expression contains all the litter inputs entering the soil, split according to the compartments at which they enter.

3.1.4 Combining transport and decomposition

In the previous sections, we analyzed the processes of diffusion, advection, and decomposition separately. Now we can combine them following the general paradigm expressed in equation 1. This general model has the form

$$
\begin{aligned}
\frac{\partial x(d, t)}{\partial t} &= \frac{\partial}{\partial d} \left(\kappa(d, t) \frac{\partial x(d, t)}{\partial d} \right) - \frac{\partial}{\partial d} f(x(d, t)) + \left\| \frac{\mathrm{d}\boldsymbol{x}(d, t)}{\mathrm{d}t} \right\|, \\
&= \frac{\partial}{\partial d} \left(\kappa(d, t) \frac{\partial x(d, t)}{\partial d} \right) - \frac{\partial}{\partial d} f(x(d, t)) + \|(\boldsymbol{u}(\boldsymbol{x}, d, t) + \mathbf{B}(\boldsymbol{x}, d, t) \cdot \boldsymbol{x}(d, t))\|.
\end{aligned} \tag{9}
$$

Most mathematical models of vertical carbon transport and decomposition should be special cases of this equation. It can lead to very complex dynamics resulting from the simultaneous effect of physical, chemical and biological processes related to transport and decomposition.

Equation 9 cannot be solved analytically, but it can be discretized in time and space to obtain numerical solutions. The discretization approach consists of defining a fixed number k of depth intervals Δd where the solution of the partial differential equation is approximated using algebraic equations, and the system is then moved forward in time at discrete intervals Δt. Most numerical methods to approximate solutions to equation 9 would attempt to find a vector $\boldsymbol{X} \in \mathbb{R}^{k+2}$ for k depth intervals by solving a linear equation of the form

$$\mathbf{A} \cdot \boldsymbol{X} = \boldsymbol{F}, \tag{10}$$

where the matrix $\mathbf{A}$ and the vector $\boldsymbol{F}$ result from the discretization of the original system using a finite-difference or a finite-element method (Lanczos, 1996; LeVeque, 2007). The dimension of this system is $(k+2) \times (k+2)$, with the 2 additional dimensions incorporating information based on the boundary conditions, which must be added to the discretized system and become an integral part of the new linear differential operator (Lanczos, 1996). Because after the discretization mass conservation must be preserved, we postulate that the new system of equations must be compartmental. In other words, a discretized system representing transport and decomposition of organic matter can be expressed as a compartmental system of the form of equation 7. There are a few examples from the previous literature that may help to confirm this assertion. For instance, Metzler et al. (2020) showed that the soil carbon module of the ELM model (Koven et al., 2013), which contains 10 discrete depth layers and 7 pools in each layer, can be approximated with a compartmental system that produces the exact same numerical solution as the original model that was developed with partial differential equations. Similarly, (Huang et al., 2018) expressed the same model of Koven et al. (2013) as a system of linear equations in matrix form and found exact approximations to the original model.

The approximation of the nonlinear model expressed with partial differential equations is possible if the system is assumed at steady-state. In the general model of equation 9, the steady state solution $x_{ss}(d)$ is obtained when $\partial x(d,t)/\partial t = 0$. At this steady-state, the amount of carbon stored in the system does not change over time and nonlinear interactions vanish. Therefore, the behavior of $x_{ss}(d)$ and a tracer such as ^{14}C, which is commonly used to parameterize SOC transport models, becomes linear with constant coefficients (Anderson, 2013). Thus, models of SOC dynamics with vertical transport can be expressed as linear systems with compartmental structure assuming the system is at near steady-state.

3.2 The constant coefficient model and its steady-state solution

Despite the generality of the model of equation (9) to represent vertical patterns of diffusion and advection, most of the models previously reported in the literature use constant diffusion and advection as well as constant decomposition and transformation rates (Table 1). Furthermore, most previous studies solve the model for the steady-state carbon content and analyze the resulting vertical patterns. Therefore, it is important to study in more detail a simplified version of the general model of equation 9 for the case of constant coefficients at the steady-state.

Assuming constant diffusion ($\kappa(d,t) = \kappa$ for all d and t), and constant flow velocity ($f(x(d,t) = v\,x(d)$, with v constant for all d and t), we can write a steady-state version of equation 9 by making the time derivative equal to zero as

$$\kappa \frac{\partial^2 x(d)}{\partial d^2} - v \frac{\partial x(d)}{\partial d} + g(d) = 0, \tag{11}$$

with $g(d)$ representing the balance between inputs and decomposition at each depth, also assuming constant decomposition and transformation rates at each depth ($\mathbf{B}(\boldsymbol{x}, d, t) = \mathbf{B}(d)$ for all $\boldsymbol{x}$, and t), and a constant vector of inputs at each depth ($\boldsymbol{u}(\boldsymbol{x}, d, t) = \boldsymbol{u}(d)$ for all $\boldsymbol{x}$ and t). Therefore,

$$g(d) = \|\boldsymbol{u}(d) + \mathbf{B}(d) \cdot \boldsymbol{x}(d)\|. \tag{12}$$

Equation 11 is a general form of a linear second order differential equation with constant coefficients, for which a numerical solution can be obtained by discretizing the system along fixed depth intervals and solving the resulting system of linear equations as in equation 10.

Two further simplified forms of the general equation can be found in the literature. The case in which advective transport is not considered relevant (e.g. O'Brien and Stout, 1978) and therefore

$$\kappa\frac{\partial^2 x(d)}{\partial d^2} + g(d) = 0, \tag{13}$$

or the case in which diffusive transport is not considered relevant (e.g. Feng et al., 1999; Baisden et al., 2002; Baisden and Parfitt, 2007)

$$-v\frac{\partial x(d)}{\partial d} + g(d) = 0. \tag{14}$$

To interpret data from pulse response experiments, some researchers have ignored the inputs and decomposition part of the model (e.g. Bruun et al., 2007) using an equation of the form

$$\kappa\frac{\partial^2 x(d)}{\partial d^2} - v\frac{\partial x(d)}{\partial d} = 0. \tag{15}$$

Models explicitly representing decomposition usually use one or three pools to represent decomposition as in most traditional first order pool models. More detailed representations of decomposition are presented in the model of Braakhekke et al. (2011, 2013), which represents five different pools, including a litter layer component clearly separating processes related to decomposition in the surface organic layer from processes more affected by vertical transport in the mineral horizons. Also, the model of Koven et al. (2013) used 7 distinct C pools: coarse woody debris, three litter pools, and three mineral soil C pools.

In the COMISSION model, not only advective DOC transport is considered, but also advective transport of litter particles similarly as in sediment models (Ahrens et al., 2015, 2020). In the latest version of the model (Ahrens et al., 2020), advective litter transfer and particle diffusion are depth dependent. The model also consider non-linear interactions among C pools, therefore it deviates from the constant linear coefficients model of equation 11 and is in better analogy to equation 9.

Table 1: Summary of models representing C dynamics along the vertical profile using the advection-diffusion-reaction paradigm. Modified and updated from Koven et al. (2013).

Model/reference	Mathematical form	d_{max} (m)	Ecosystem/location	n	v	κ	Péclet number
O'Brien and Stout (1978)	Eq. 13	1.00	Managed pasture, NZ	1		13.2 cm^2 yr^{-1}	0
Elzein and Balesdent (1995)	Eq. 11	1.65	Kattinkar, India	3	0.13 mm yr^{-1}	5.15 cm^2 yr^{-1}	0.003
Elzein and Balesdent (1995)	Eq. 11	1.95	Pará, Brazil	3	0.34 mm yr^{-1}	16.58 cm^2 yr^{-1}	0.002
Elzein and Balesdent (1995)	Eq. 11	1.63	Bahia, Brazil	3	0.48 mm yr^{-1}	5.29 cm^2 yr^{-1}	0.009
Elzein and Balesdent (1995)	Eq. 11	0.52	Forest, Bezange, France	3	0.6 mm yr^{-1}	0.94 cm^2 yr^{-1}	0.064
Elzein and Balesdent (1995)	Eq. 11	1.00	Forest, Marly, France	3	0.42 mm yr^{-1}	1.48 cm^2 yr^{-1}	0.028
Feng et al. (1999)	Eq. 14	1.00	Oak chaparral, USA	1	1.51 cm yr^{-1}		∞
Feng et al. (1999)	Eq. 14	1.00	Pine, USA	1	1.67 cm yr^{-1}		∞
Feng et al. (1999)	Eq. 14	1.00	Ceanothus chaparral, USA	1	1.56 cm yr^{-1}		∞
Feng et al. (1999)	Eq. 14	1.00	Chamise chaparral, USA	1	1.52 cm yr^{-1}		∞
Baisden et al. (2002) [1]	Eq. 14		< 3 ky old grassland soil, USA	3	[4.0, 0.47, 0.40] mm yr^{-1}		∞
Baisden et al. (2002)	Eq. 14		200 ky old grassland soil, USA	3	[4.0, 0.49, 0.39] mm yr^{-1}		∞
Baisden et al. (2002)	Eq. 14		600 ky old grassland soil, USA	3	[3.2, 0.28, 0.43] mm yr^{-1}		∞
Baisden et al. (2002)	Eq. 14		3 My old grassland soil, USA	3	[0.5, 0.26, 0.10] mm yr^{-1}		∞
Bruun et al. (2007)	Eq. 15	0.55	Cropland, Denmark	0	0.0081 cm yr^{-1}	0.71 cm^2 yr^{-1}	0.011
Baisden and Parfitt (2007)	Eq. 14	1.00	15 ky old grassland soil, NZ	3	[6.2, 0.9, 0.19] mm yr^{-1}		∞
Baisden and Parfitt (2007)	Eq. 14	1.00	200 ky old grassland soil, NZ	3	[0.6, 1.3, 0.25] mm yr^{-1}		∞
Baisden and Parfitt (2007)	Eq. 14	1.00	600 ky old grassland soil, NZ	3	[0.5, 0.5, 0.5] mm yr^{-1}		∞
Braakhekke et al. (2011)	Eq. 11	0.7	Deciduous forest, Germany	5	0.002 m yr^{-1}	0.6 cm^2 yr^{-1} [2]	0.333
Braakhekke et al. (2013)	Eq. 11	2.0	Pine forest, Netherlands	5	0.0651 m yr^{-1}	0.0852 cm^2 yr^{-1}	76.402
Braakhekke et al. (2013)	Eq. 11	0.7	Deciduous forest, Germany	5	0.00137 m yr^{-1}	0.6792 cm^2 yr^{-1}	0.202
Koven et al. (2013)	Eq. 13	3.8	Global, non-permafrost	7		1 cm^2 yr^{-1}	0
Ahrens et al. (2015)	Eq. 11	0.9	Coniferous forest, Germany	4	NA	3.24×10^{-10} m^2 s^{-1}	NA

[1] The model considers three separate values of v for each C pool
[2] Assuming a bulk density of 1000 kg cm^{-3}

474   Particularly interesting is the model of Elzein and Balesdent (1995), which follows the form of
475   equation 11 and includes advection, diffusion, and decomposition of three distinct pools. This model
476   is rather useful because it includes a minimum of complexity to represent most relevant processes of
477   a carbon transport model. It is also a useful model for parameterization against data on C and ^{14}C
478   concentrations in vertical profiles.

479   Returning to our steady-state analysis of the constant coefficient model, we can solve the system
480   for the first derivative and analyze individual components of this equation

$$\frac{\partial x(d)}{\partial d} = \frac{\kappa}{v}\frac{\partial^2 x(d)}{\partial d^2} + \frac{g(d)}{v}. \tag{16}$$

481   For the special case of one single pool with vertical root inputs represented by $u(d)$ and vertical
482   decomposition rates by $k(d)$,

$$\frac{\partial x(d)}{\partial d} = \frac{\kappa}{v}\frac{\partial^2 x(d)}{\partial d^2} + \frac{u(d) - k(d)x(d)}{v}. \tag{17}$$

483   Equation 17 is very useful to analyze the shape of soil C profiles for cases in which the equilibrium
484   assumption is reasonable. First, equation 17 shows that the vertical change of C in a soil profile is
485   inversely proportional to the advective movement of C such as in the case of DOC transport. For large
486   values of advection velocity (v) the rate of change of C by depth would be small and the vertical C
487   profile would resemble a vertical line. Second, the sign of the rate of change of C by depth is mostly
488   determined by the difference between belowground C inputs and decomposition. At depths where
489   the decomposition flux ($k(d)\ x(d)$) is larger than belowground inputs, the decrease of C by depth is
490   maximum (maximum negative value). Third, the ratio between diffusion and advection velocity (κ/v),
491   the inverse of the Péclet number (see below), influences how second order transport processes affect
492   the shape of the rate of change of the vertical C profile (Figure 1).

493   In the analysis of partial differential equations, the Péclet number, defined as the ratio of advection
494   to diffusion, plays a very important role in determining characteristics of the solution such as its
495   numerical stability (LeVeque, 2007). In addition, the Péclet number can be used to determine the
496   degree by which diffusion or advection may dominate the shape of a soil C profile (Figure 1).

497   If soil C always decreases with depth (Jobbágy and Jackson, 2000), the decomposition flux in
498   equation 17 must be dominant across the entire soil profile so the rate of change with depth remains
499   negative. In fact, this analysis suggests that the balance between lateral C inputs and decomposition
500   is one of the main factors that affect the shape of soil C profiles where a continuous decrease in soil C
501   is commonly observed.

502   A corollary or implication provided by equation 17 is that if the decrease in soil C with depth
503   follows a simple exponential function, the right hand side of equation 17 must be a constant value
504   for all depths. This situation seems unlikely given the different interacting process that occur in a
505   soil, and in fact, mathematical functions different than the simple exponential provide the best fit to
506   observed data (Jobbágy and Jackson, 2000).

3.3   Numerical example

508   We used equation 17 to investigate the role of diffusion, advection, decomposition and lateral inputs
509   on the shape of idealized soil carbon profiles. We chose values of κ and v within the range of values
510   obtained in previous models (Table 1) as well as representative functions for $k(d)$ and $u(d)$ within the
511   range of previous studies (e.g. Elzein and Balesdent, 1995; Jackson et al., 1996, 1997; Koven et al.,
512   2013).

513   To investigate the effect of diffusion and advection, we ran simulations with values of $\kappa = \{0.1, 1, 5, 15\}$
514   cm^2 yr^{-1} and $v = \{0.1, 1, 5, 10\}$ cm yr^{-1} (Figure 2). The results show that vertical transport processes
515   tend to create a horizon with largest rate of change in concentrations of C with depth (1st derivative)
516   close to the surface. This layer could be the result of either advection or diffusion (Figure 2). Because
517   in these simulations, lateral root inputs and decomposition decrease with depth (see below), there is
518   a general trend of C concentrations to decline to values close to zero. Therefore, vertical transport do
519   not seem to play a major role in transporting carbon below 50 cm depth within the range of advection

and diffusion values used in these simulations. Only at high advection velocities ($v = 10$ cm yr^{-1}) some carbon is transported below 50 cm depth, but this advection velocity is much higher than what has been used before in other models (Table 1).

The first derivative of the C concentration profiles with respect to depth from these simulations (Figure 2 right panels), showed negative derivatives for the entire depth profile. According to equation 17, the first derivative can only be positive if lateral root inputs and transport processes dominate over the decomposition flux, which is not the case in these simulations. The decomposition flux dominates over all other processes making the first derivative negative although approaching zero at deeper layers. As advection velocity increased, the first derivatives were less negative, indicating that as advective transport increases the change in C concentrations by depth is less pronounced.

In a second set of simulations, we practically removed advection and diffusion by making the value of these coefficients very small ($\kappa = v = 0.01$) and represented lateral root inputs with the function

$$u(d) = -\beta^d \, \ln \beta. \tag{18}$$

This function predicts vertical root distributions and was originally proposed by Gale and Grigal (1987) and used by Jackson et al. (1996, 1997) to obtain vertical root distributions at the biome level. The original function predicts the fraction of root biomass for each depth, and multiplied by an average root turnover rate of 1 yr^{-1} (Gill and Jackson, 2000), gives the proportion of root inputs per depth interval $u(d)$. For the simulations, we used values of $\beta : \{0.92, 0.95, 0.98\}$ that include the observed extremes of values for shallow root systems ($\beta = 0.92$) and deep root systems ($\beta = 0.98$) (Gale and Grigal, 1987; Jackson et al., 1996).

The function used to represent decomposition rates by depth was extracted from Koven et al. (2013)

$$k(d) = k_0 \exp\left(\frac{-d}{d_e}\right), \tag{19}$$

with the maximum decomposition rate at the surface given by $k_0 = k(d = 0)$, and d_e representing the e-folding depth of decomposition rates. In our simulations, we used values of $k_0 : \{1, 0.1, 0.01\}$ yr^{-1} and a constant value of $d_e = 90$ cm (the model showed little sensitivity to different values of d_e).

The results from this second set of simulations evaluating the effect of lateral root inputs and decomposition showed that slowing down decomposition can have a significant effect on the shape of the vertical soil C profile. These results seems counterintuitive because equation 17 suggest that the negative term of the equation should be affected by larger values of $k(d)$, but because with slow decomposition higher amounts of C are obtained at steady-state, the entire term $k(d)x(d)$ is large, promoting a strong soil C gradient. The vertical distribution of root inputs has also a significant effect on the shape of the soil C profile, with shallow root inputs promoting a strong vertical gradient and deep rooting systems a more pronounced gradient with lower values of the first derivative. In this set of simulations, we observed also a maximum rate of change of C at the upper layers where the value of the first derivative reached a maximum.

4 Assessing C sequestration and the fate of new C inputs

4.1 Fate, transit time, and carbon sequestration in the subsoil

In the context of climate change mitigation, we are generally interested in evaluating the capacity of soils for storing carbon at relevant timescales associated with management and policy outcomes. In many cases we are interesting in comparing different soils; and in other cases, we are interested in evaluating the effectiveness of different soil management practices. In any case, we need to use appropriate metrics to evaluate the environmental benefit of carbon sequestration.

If we aim at promoting soil C sequestration, it is then important to analyze the fate of new inputs entering the soil, assess for how long the new carbon remains stored, and how much warming can be avoided while the C is stored (Sierra et al., 2021a; Crow and Sierra, 2022). For this purpose, we can use the following metrics: fate, transit time, and carbon sequestration, which are mathematically defined as follows.

For a compartmental system in equilibrium, where carbon inputs are balanced with C losses, the fate of C entering at a time t_0 can be obtained as a function that predicts the mass of C remaining in the soil at any given time $t > t_0$ (Sierra et al., 2021b)

$$\boldsymbol{M}(t) = e^{\tau \mathbf{B}} \, \boldsymbol{u}, \tag{20}$$

where $\boldsymbol{M}(t)$ is a vector with the mass remaining for each compartment. This mass remaining is related to the transit time of carbon, which is defined as the time it takes carbon atoms to pass through the entire network of compartments until C leaves the soil system (Bolin and Rodhe, 1973; Manzoni et al., 2009; Sierra et al., 2018a). It can be expressed as (Metzler and Sierra, 2018)

$$f_T(\tau) = -\mathbf{1}^\top \, \mathbf{B} \, e^{\tau \mathbf{B}} \frac{\boldsymbol{u}}{\|\boldsymbol{u}\|} \tag{21}$$

Carbon Sequestration (CS) evaluates the fate of new inputs entering the soil integrated over a period of time. The amount of sequestration quantified by the CS metric depends on both the amount of inputs entering the soil and the time it takes this carbon to return to the atmosphere in the form of respiration. This amount of time is proportional to the transit time of carbon.

For a compartmental system at equilibrium, CS can be obtained as

$$\mathrm{CS}(t) = \int_{t_0}^{t} \|e^{\tau \, \mathbf{B}} \, \boldsymbol{u}\| \mathrm{d}\tau, \tag{22}$$

which is the integral of the total amount of mass remaining in the soil from a cohort of inputs entering at t_0.

If a particular transport-decomposition model can be discretized and expressed as a compartmental system following standard numerical methods (LeVeque, 2007; Lanczos, 1996), one can use equation 22 to quantify the fate, transit time and CS of a particular soil and compare results with those from another soil, or with the outcomes of different forms of management.

Alternatively, $\boldsymbol{M}(t)$ and $f_T(\tau)$ can be obtained using impulse response experiments with existing transport models that are difficult to express as a compartmental system (Thompson and Randerson, 1999; Metzler and Sierra, 2018). The approach consists of running a model until reaching equilibrium, and at this point add a pulse of carbon and observe the mass remaining of the pulse over time, which is an approximation to $\boldsymbol{M}(t)$. One can also observe the respiration flux after the addition of the pulse, which is an approximation to the transit time distribution $f_T(\tau)$ (Metzler and Sierra, 2018). The results from pulse-response experiments should provide very valuable information to assess the fate of new inputs entering the soil and whether they remain for relevant periods of time.

4.2   Numerical example

In the previous example, we saw that transport, decomposition, and lateral root inputs play an important role in determining the shape of soil C profiles at equilibrium. We evaluate now with an example how fast/slow transport, combined with fast/slow decomposition in soil profiles can affect the fate, transit time and carbon sequestration of a soil. Our aim is to assess the fate of new carbon inputs and whether they remain in soil for timescales relevant for climate change mitigation.

Given that our previous example showed that diffusion plays a minor role in comparison to advection for moving carbon downwards, we set a fixed value of $\kappa = 1$ cm^2 yr^{-1} and varied the values of v. For simulations with fast transport, the values were $v = 5$ cm yr^{-1}, and for simulations with slow transport $v = 0.1$ cm yr^{-1}. Decomposition rates were considered fast with values of $k_0 = 1$ yr^{-1} and slow with $k_0 = 0.1$ yr^{-1} at the surface (Table 2) and declining with depth according to equation 19. In all simulations, we considered a root input profile with an intermediate value of $\beta = 0.95$, i.e. not too shallow nor too deep roots.

Simulation results showed that most C inputs entering at any given time only stay in the soil a few years, and only under slow decomposition, some C may remain for a few decades (Figure 4, Table 2). Decomposition rates seem to play a stronger control on the fate of C inputs than vertical transport rates. Under fast decomposition, most carbon was lost in 5 years independently from

Table 2: Parameters used and results obtained for simulations evaluating the effect of transport and decomposition on the fate, transit time and carbon sequestration of new inputs. Tf–DF: transport fast, decomposition fast; Tf–Ds: transport fast, decomposition slow; Ts–Df: transport slow, decomposition fast; Ts-Ds: transport slow, decomposition slow.

	Tf–Df	Tf–Ds	Ts–Df	Ts–Ds
κ (cm^2 yr^{-1})	1.000	1.000	1.000	1.000
v (cm yr^{-1})	5.000	5.000	0.100	0.100
k_0 (yr^{-1})	1.000	0.100	1.000	0.100
β	0.950	0.950	0.950	0.950
Proportion remaining after 1 yr	0.449	0.914	0.424	0.875
Proportion remaining after 10 yr	0.002	0.480	0.001	0.392
Proportion remaining after 50 yr	0.000	0.000	0.000	0.022
Mean transit time (yr^{-1})	1.333	9.699	1.217	11.498
Median transit time (yr^{-1})	0.859	9.444	0.799	7.096
CS($t \to \infty$)	16.028	363.721	12.587	133.416

609 transport velocity, and very small proportions travelled through the soil profile because the carbon
610 was decomposed before it had a chance to move downwards. Under slow decomposition and fast
611 transport, some carbon is preserved longer because it decomposes at slower rates at deeper layers, but
612 eventually this transported carbon is also decomposed in a few decades (Figure 4).

613   The transit time distribution of C through the entire soil profile for these different simulations
614 showed that the large majority of C entering the soil at any given time is lost within the first year
615 (Figure 5a). Fifty percent of the C that enters the soil is lost in 0.86 years in the scenario with fast
616 decomposition and fast transport, while in the scenario with slow decomposition and fast transport
617 50% of the new carbon is lost in 9.4 years (Table 2). The slow decomposition scenarios showed a very
618 different tail in the transit time distribution compared to the fast decomposition scenarios, with a
619 larger proportion of carbon staying for longer times under slow decomposition. Therefore, the mean
620 transit time is influenced by these long tails, with the mean transit time in the fast transport slow
621 decomposition scenario of 1.3 years, and 11.5 years in the slow transport slow decomposition scenario
622 (Table 2a). Despite slow decomposition however, most of the new inputs do not stay for timescales
623 beyond a few decades at the maximum.

624   At steady-state, significantly more carbon is stored in the case of slow decomposition, particularly
625 in the scenario of fast transport and slow decomposition (Figure 5b). However, to reach this large
626 steady-state C concentrations, very long timescales of carbon accumulation are required. According to
627 the transit time distributions, very small amounts of new C inputs remain in the long-term, therefore
628 it would take a considerably long time (beyond decades) to reach these steady-state C values.

5   Empirical evidence from soil profiles

630 The two numerical examples from the previous section suggest that (i) the change of soil C with depth
631 is largely influenced by the difference between root inputs and decomposition, and to a lesser degree
632 by vertical transport processes such as diffusion and advection; (ii) most new carbon inputs entering
633 the soil do not remain stored for long timescales. In the following section, we will explore global-scale
634 datasets of soil C profiles to test whether these theoretical model predictions have empirical support
635 on observations.

5.1   The shape of the vertical C profile across regions

637 The International Soil Radiocarbon Database (ISRaD) is a comprehensive and well curated collection
638 of soil carbon and radiocarbon data (Lawrence et al., 2020). We used version 1.7.8 of the database
639 and extracted information on soil C concentration with depth down to 1 m. Data from 600 individual
640 profiles were grouped by Köppen-Geiger climate zones (Beck et al., 2018) and averaged by 1 cm depth

641 increments. Volcanic soils (classified as such in the field) were treated as a separate group given their
642 distinct vertical C profile. A mass-preserving spline function (equal-area quadratic smoothing spline)
643 was applied to each profile to account for the varying depth intervals in which samples across profiles
644 were taken (Ponce-Hernandez et al., 1986; Bishop et al., 1999). This spline function interpolates C
645 concentration for a continuum of depths, i.e. an approximation to the function $x(d)$ for each of the
646 groups (Figure 6).

647   Soil carbon decreased rapidly with depth in most soil profiles reaching values close to zero at 1 m
648 depth (Figure 6), with the exception of soils from tundra/polar regions and volcanic soils, which still
649 contain relatively large quantities of C at 90 cm depth. Please note that these values are reported
650 as concentrations with respect to mass of soil. Bulk density data is not commonly reported for
651 individual profiles and much less for individual depth horizons. Therefore, comparisons with the
652 simulation experiments from previous sections must be done only with respect to qualitative aspects
653 and not with respect to quantitative values.

654   The first derivative of soil C concentrations with respect to depth ($\partial x(d)/\partial d$, Figure 7) was negative
655 for all groups, indicating that soil C always decreases with depth for these aggregated profiles. This
656 is in agreement with our previous simulations in which the first derivatives were always negative. We
657 observed for all groups a peak in the first derivative where it reaches a maximum negative value,
658 indicating that soil C decreases more strongly at some intermediate depth between 10 and 20 cm
659 (Figure 7). According to equation 17, a maximum negative value of the first derivative can only
660 occur at depths where the microbial decomposition flux ($k(d)x(d)$) has its maximum value, i.e. when
661 microbes are consuming the maximum amount of carbon possible.

662   The value of the first derivative had the largest values overall for volcanic soils, and the lowest
663 values for arid soils. In both cases decomposition rates may be slow compared to other soils; in
664 volcanic soils the presence of amorphous non-crystalline surfaces promote sorption of organic matter
665 to minerals and therefore slow decomposition and strong C accumulation (Marin-Spiotta et al., 2011;
666 Crow et al., 2015); in arid soils low moisture availability leads to slow decomposition rates, but also low
667 primary productivity leads to low carbon stocks (Moyano et al., 2013; Sierra et al., 2015). Therefore,
668 negative values of the first derivative are strongly dependent on the C stocks ($x(d)$), and to a lesser
669 extend on the decomposition rate ($k(d)$). The decomposition rate obviously plays a major role in
670 determine the size of the C stock in conjunction with the input fluxes at depth, but the rate of decline
671 of C with depth is mostly influenced by the resulting C stock. In addition, the last term of equation
672 17 also reveals that for systems with slow advection velocities v approaching zero, small differences
673 between lateral inputs and decomposition may be amplified. In other words, the large values of the
674 negative derivative for the volcanic soils may be the result of very low advective movement of DOC,
675 amplifying small differences between lateral inputs and decomposition.

676   Overall, the data from soil C profiles aggregated by regional groups and volcanic soils provide
677 evidence supporting the idea that vertical transport may play a secondary role in determining the rate
678 of soil C decrease with depth. The difference between lateral root inputs and decomposition may play
679 a primary role in determining the shape of soil C profiles, and this difference may be amplified at low
680 advection velocity rates. Diffusive movement of soil C seems to play a small role in these aggregated
681 groups, something suggested by the low values of the second derivative (Figure 7); however, diffusion
682 may have some control on the peak of C decrease found close to the surface in these profiles.

5.2   Transit times of C from vertical profiles

684 Using data from ISRaD and a dataset on root input profiles, Xiao et al. (2022) obtained estimates of
685 mean ages and mean transit times for soil C profiles at the global scale. The global averages revealed
686 that mean transit times of C are always younger than the mean age of C stored at all soil depths
687 (Figure 8). In other words, despite the C stored in the soil being hundreds to thousands of years
688 old, the C respired is only a few years to decades old. This result is consistent with our transit time
689 simulations that showed mean transit times of only a few years (Figure 5, Table 2). However, the
690 actual values of mean transit time obtained from the data are actually much higher than those from
691 the model results. This is to be expected given that the model used for the example only considered
692 one single pool, but in reality soil carbon is highly heterogeneous and a significant proportion of its

total carbon cycles at much slower rates, which would contribute to higher transit times. In addition, sorption of OM to mineral surfaces may increase with depth, making the overall decomposition of C at depth more limited (Ahrens et al., 2020). Nevertheless, model simulations and observations agree in that new C inputs to soil only remain stored in timescales of years to decades.

Fast mean transit times were observed for tropical forest, grassland and cropland soils, while long transit times in the order of decades to centuries were only observed for tundra and boreal forest soils (Figure 8). These results are consistent with the idea that low temperatures and energy limitation may play a significant role in controlling the transit time of C at the biome level (Lu et al., 2018; Xiao et al., 2022), with fast transit times in warm regions and longer transit times in cold high-latitude regions.

Because transit times are directly related to Carbon Sequestration CS (equations 21 and 22), we expect only tundra and boreal forest soils to store C in the subsoil at timescales relevant for climate change mitigation, i.e. in the order of decades to centuries. In fact, previous studies have found that a large proportion of carbon used by microorganisms in the subsoil is recent and does not contribute to C stabilization in the subsoil (Balesdent et al., 2018; Scheibe et al., 2023). Therefore, we would expect lower values of CS for tropical forests, grasslands and cropland soils in comparison with boreal forests and tundra soils. However, it is important to keep in mind that productivity in these high-latitude regions is relatively low compared to temperate and equatorial latitudes (Xiao et al., 2023). CS as defined in equation 22 accounts for this trade-off between the amount of inputs and its transit time through the soil, and it can be used to more specifically assess the climate mitigation potential of specific amounts of C added to the soil.

6   Summary and conclusions

We reviewed the main processes that contribute to the formation of soil C profiles, and the mathematical models that are used to represent them. Our main findings were: 1. The main processes that contribute to the formation of soil C profiles are root productivity and rhizodeposition, microbial decomposition, advective processes such as liquid phase transport, and diffusive processes such as bioturbation and cryoturbation. 2. These processes can be expressed in models under the general paradigm of the advection-diffusion-reaction equation, with most previously proposed models being a special case of this general paradigm. 3. Advective and diffusive processes seem to be of secondary importance in explaining the shape of vertical soil C profiles. The difference between vertical carbon inputs and decomposition seems to play a primary role in explaining the decline of soil C with depth. 4. The transit time of C is only a few years to decades in most soils, which implies that promoting the addition of new C inputs to soils would only contribute to climate change mitigation in the short term (years to decades). Carbon sequestration at longer timescales is only possible in slow cycling systems such as tundra and boreal forest soils, but primary production is relatively low in these regions.

Although soils store large quantities of C in the subsoil and this carbon is hundreds to thousands of years old, our review suggest that new carbon that enters the soil is cycled quickly by the activity of microorganisms with relatively fast transit times. Therefore, promoting new C inputs to subsoil may not have a significant contribution to climate change mitigation as it could be inferred from carbon stocks and ages in the subsoil alone. Conservation of existing subsoil C stocks seems to be a more relevant and important aspect because the timescales required to form existing soil C stocks were on the order of centuries to millenia and there are important risks that through land use change, or non-sustainable agricultural practices, important portions of these existing stocks may be lost quickly.

Acknowledgements

Data availability and reproducibility of results

All code and data required to reproduce the results of this manuscript is available at `https://github.com/MPIBGC-TEE/subsoilCseq`. Upon acceptance, all files will be archived in Zenodo with a corresponding digital object identifier.

References

Ahrens, B., Braakhekke, M. C., Guggenberger, G., Schrumpf, M., and Reichstein, M. (2015). Contribution of sorption, DOC transport and microbial interactions to the ^{14}C age of a soil organic carbon profile: Insights from a calibrated process model. *Soil Biology and Biochemistry*, 88:390 – 402.

Ahrens, B., Guggenberger, G., Rethemeyer, J., John, S., Marschner, B., Heinze, S., Angst, G., Mueller, C. W., Kögel-Knabner, I., Leuschner, C., Hertel, D., Bachmann, J., Reichstein, M., and Schrumpf, M. (2020). Combination of energy limitation and sorption capacity explains 14c depth gradients. *Soil Biology and Biochemistry*, 148:107912.

Alban, D. H. and Berry, E. C. (1994). Effects of earthworm invasion on morphology, carbon, and nitrogen of a forest soil. *Applied Soil Ecology*, 1(3):243–249.

Allison, S. D., Wallenstein, M. D., and Bradford, M. A. (2010). Soil-carbon response to warming dependent on microbial physiology. *Nature Geosci*, 3(5):336–340. 10.1038/ngeo846.

Amos, B. and Walters, D. T. (2006). Maize root biomass and net rhizodeposited carbon. *Soil Science Society of America Journal*, 70(5):1489–1503.

Anderson, D. H. (2013). *Compartmental modeling and tracer kinetics*, volume 50. Springer Science & Business Media.

Anderson, L. J., Comas, L. H., Lakso, A. N., and Eissenstat, D. M. (2003). Multiple risk factors in root survivorship: a 4-year study in concord grape. *New Phytologist*, 158(3):489–501.

Arndt, S., Jørgensen, B. B., LaRowe, D. E., Middelburg, J. J., Pancost, R. D., and Regnier, P. (2013). Quantifying the degradation of organic matter in marine sediments: A review and synthesis. *Earth-Science Reviews*, 123(0):53–86.

Baisden, W. and Parfitt, R. (2007). Bomb 14C enrichment indicates decadal C pool in deep soil? *Biogeochemistry*, 85(1):59–68.

Baisden, W. T., Amundson, R., Brenner, D. L., Cook, A. C., Kendall, C., and Harden, J. W. (2002). A multiisotope c and n modeling analysis of soil organic matter turnover and transport as a function of soil depth in a california annual grassland soil chronosequence. *Global Biogeochem. Cycles*, 16(4):1135.

Balesdent, J., Basile-Doelsch, I., Chadoeuf, J., Cornu, S., Derrien, D., Fekiacova, Z., and Hatté, C. (2018). Atmosphere–soil carbon transfer as a function of soil depth. *Nature*, 559(7715):599–602.

Beck, H. E., Zimmermann, N. E., McVicar, T. R., Vergopolan, N., Berg, A., and Wood, E. F. (2018). Present and future köppen-geiger climate classification maps at 1-km resolution. *Scientific Data*, 5(1):180214.

Bishop, T., McBratney, A., and Laslett, G. (1999). Modelling soil attribute depth functions with equal-area quadratic smoothing splines. *Geoderma*, 91(1):27–45.

Bohlen, P. J., Pelletier, D. M., Groffman, P. M., Fahey, T. J., and Fisk, M. C. (2004). Influence of earthworm invasion on redistribution and retention of soil carbon and nitrogen in northern temperate forests. *Ecosystems*, 7(1):13–27.

Bolin, B. and Rodhe, H. (1973). A note on the concepts of age distribution and transit time in natural reservoirs. *Tellus*, 25(1):58–62.

Bolinder, M., Janzen, H., Gregorich, E., Angers, D., and VandenBygaart, A. (2007). An approach for estimating net primary productivity and annual carbon inputs to soil for common agricultural crops in canada. *Agriculture, Ecosystems & Environment*, 118(1):29–42.

Bolinder, M. A., Crotty, F., Elsen, A., Frac, M., Kismányoky, T., Lipiec, J., Tits, M., Tóth, Z., and Kätterer, T. (2020). The effect of crop residues, cover crops, manures and nitrogen fertilization on soil organic carbon changes in agroecosystems: a synthesis of reviews. *Mitigation and Adaptation Strategies for Global Change*, 25(6):929–952.

Börjesson, G., Bolinder, M. A., Kirchmann, H., and Kätterer, T. (2018). Organic carbon stocks in topsoil and subsoil in long-term ley and cereal monoculture rotations. *Biology and Fertility of Soils*, 54(4):549–558.

Bosatta, E. and Ågren, G. I. (1996). Theoretical analyses of carbon and nutrient dynamics in soil profiles. *Soil Biology and Biochemistry*, 28(10–11):1523 – 1531.

Boudreau, B. P. (1986a). Mathematics of tracer mixing in sediments; i, spatially-dependent, diffusive mixing. *American Journal of Science*, 286(3):161–198.

Boudreau, B. P. (1986b). Mathematics of tracer mixing in sediments; ii, nonlocal mixing and biological conveyor-belt phenomena. *American Journal of Science*, 286(3):199–238.

Boudreau, B. P. (1989). The diffusion and telegraph equations in diagenetic modelling. *Geochimica et Cosmochimica Acta*, 53(8):1857–1866.

Braakhekke, M. C., Beer, C., Hoosbeek, M. R., Reichstein, M., Kruijt, B., Schrumpf, M., and Kabat, P. (2011). Somprof: A vertically explicit soil organic matter model. *Ecological Modelling*, 222(10):1712–1730.

Braakhekke, M. C., Wutzler, T., Beer, C., Kattge, J., Schrumpf, M., Ahrens, B., Schöning, I., Hoosbeek, M. R., Kruijt, B., Kabat, P., and Reichstein, M. (2013). Modeling the vertical soil organic matter profile using bayesian parameter estimation. *Biogeosciences*, 10(1):399–420.

Brovelli, A., Batlle-Aguilar, J., and Barry, D. (2012). Analysis of carbon and nitrogen dynamics in riparian soils: Model development. *Science of The Total Environment*, 429:231–245. Special Section - Arsenic in Latin America, An Unrevealed Continent: Occurence, Health Effects and Mitigation.

Bruun, S., Christensen, B. T., Thomsen, I. K., Jensen, E. S., and Jensen, L. S. (2007). Modeling vertical movement of organic matter in a soil incubated for 41 years with 14c labeled straw. *Soil Biology and Biochemistry*, 39(1):368 – 371.

Bunzl, K. (2002). Transport of fallout radiocesium in the soil by bioturbation: a random walk model and application to a forest soil with a high abundance of earthworms. *Science of The Total Environment*, 293(1):191–200.

Button, E. S., Pett-Ridge, J., Murphy, D. V., Kuzyakov, Y., Chadwick, D. R., and Jones, D. L. (2022). Deep-c storage: Biological, chemical and physical strategies to enhance carbon stocks in agricultural subsoils. *Soil Biology and Biochemistry*, 170:108697.

Carter, M. and Gregorich, E. (2010). Carbon and nitrogen storage by deep-rooted tall fescue (lolium arundinaceum) in the surface and subsurface soil of a fine sandy loam in eastern canada. *Agriculture, Ecosystems & Environment*, 136(1):125–132.

Chabbi, A., Kögel-Knabner, I., and Rumpel, C. (2009). Stabilised carbon in subsoil horizons is located in spatially distinct parts of the soil profile. *Soil Biology and Biochemistry*, 41(2):256–261.

Chantigny, M. H. (2003). Dissolved and water-extractable organic matter in soils: a review on the influence of land use and management practices. *Geoderma*, 113(3):357–380. Ecological aspects of dissolved organic matter in soils.

Chapin, F., Matson, P., and Mooney, H. A. (2002). *Principles of terrestrial ecosystem ecology*. Springer Veralg, New York.

Chen, S., Martin, M. P., Saby, N. P., Walter, C., Angers, D. A., and Arrouays, D. (2018). Fine resolution map of top- and subsoil carbon sequestration potential in france. *Science of The Total Environment*, 630:389–400.

Chenu, C., Angers, D. A., Barré, P., Derrien, D., Arrouays, D., and Balesdent, J. (2019). Increasing organic stocks in agricultural soils: Knowledge gaps and potential innovations. *Soil and Tillage Research*, 188:41–52. Soil Carbon and Climate Change: the 4 per Mille Initiative.

Choi, J., Francois-Carcaillet, F., and Boudreau, B. P. (2002). Lattice-automaton bioturbation simulator (labs): implementation for small deposit feeders. *Computers & Geosciences*, 28(2):213–222.

Clark, D., Brown, S., Klicklighter, D., Chambers, J., Tomlinson, J., and Ni, J. (2001). Measuring net primary production in forests: concepts and field methods. *Ecological Applications*, 11(2):356–370.

Collins, H., Smith, J., Fransen, S., Alva, A., Kruger, C., and Granatstein, D. (2010). Carbon sequestration under irrigated switchgrass (panicum virgatum l.) production. *Soil Science Society of America Journal*, 74(6):2049–2058.

Crow, S., Reeves, M., Schubert, O., and Sierra, C. (2015). Optimization of method to quantify soil organic matter dynamics and carbon sequestration potential in volcanic ash soils. *Biogeochemistry*, 123(1-2):27–47.

Crow, S. E. and Sierra, C. A. (2022). The climate benefit of sequestration in soils for warming mitigation. *Biogeochemistry*, 161:71–84.

Dal Ferro, N., Piccoli, I., Berti, A., Polese, R., and Morari, F. (2020). Organic carbon storage potential in deep agricultural soil layers: Evidence from long-term experiments in northeast italy. *Agriculture, Ecosystems & Environment*, 300:106967.

Don, A., Rödenbeck, C., and Gleixner, G. (2013). Unexpected control of soil carbon turnover by soil carbon concentration. *Environmental Chemistry Letters*, pages 1–7.

Dörr, H. and Münnich, K. O. (1989). Downward movement of soil organic matter and its influence on trace-element transport (210pb, 137cs) in the soil. *Radiocarbon*, 31(3):655–663.

Ehleringer, J., Buchmann, N., and Flanagan, L. B. (2000). Carbon isotope ratios in belowground carbon cycle processes. *Ecological Application*, 10(2):412–422.

Elzein, A. and Balesdent, J. (1995). Mechanistic simulation of vertical distribution of carbon concentrations and residence times in soils. *Soil Sci. Soc. Am. J.*, 59(5):1328–1335.

Eusterhues, K., Rumpel, C., Kleber, M., and Kögel-Knabner, I. (2003). Stabilisation of soil organic matter by interactions with minerals as revealed by mineral dissolution and oxidative degradation. *Organic Geochemistry*, 34(12):1591–1600.

Fan, J., McConkey, B., Wang, H., and Janzen, H. (2016). Root distribution by depth for temperate agricultural crops. *Field Crops Research*, 189:68–74.

Feng, X., Peterson, J. C., Quideau, S. A., Virginia, R. A., Graham, R. C., Sonder, L. J., and Chadwick, O. A. (1999). Distribution, accumulation, and fluxes of soil carbon in four monoculture lysimeters at san dimas experimental forest, california. *Geochimica et Cosmochimica Acta*, 63(9):1319–1333.

Freier, K. P., GLASER, B., and ZECH, W. (2010). Mathematical modeling of soil carbon turnover in natural Podocarpus forest and eucalyptus plantation in ethiopia using compound specific δ13C analysis. *Global Change Biology*, 16(5):1487–1502.

Gale, M. R. and Grigal, D. F. (1987). Vertical root distributions of northern tree species in relation to successional status. *Canadian Journal of Forest Research*, 17(8):829–834.

Gaudinski, J. B., Torn, M. S., Riley, W. J., Dawson, T. E., Joslin, J. D., and Majdi, H. (2010). Measuring and modeling the spectrum of fine-root turnover times in three forests using isotopes, minirhizotrons, and the radix model. *Global Biogeochem. Cycles*, 24(3):GB3029.

Gill, R. A. and Jackson, R. B. (2000). Global patterns of root turnover for terrestrial ecosystems. *New Phytologist*, 147(1):13–31.

Gjettermann, B., Styczen, M., Hansen, H. C. B., Vinther, F. P., and Hansen, S. (2008). Challenges in modelling dissolved organic matter dynamics in agricultural soil using daisy. *Soil Biology and Biochemistry*, 40(6):1506–1518. Special Section: Functional Microbial Ecology: Molecular Approaches to Microbial Ecology and Microbial Habitats.

Grant, R., Juma, N., and McGill, W. (1993). Simulation of carbon and nitrogen transformations in soil: Mineralization. *Soil Biology and Biochemistry*, 25(10):1317–1329.

Guan, X.-K., Turner, N. C., Song, L., Gu, Y.-J., Wang, T.-C., and Li, F.-M. (2016). Soil carbon sequestration by three perennial legume pastures is greater in deeper soil layers than in the surface soil. *Biogeosciences*, 13(2):527–534.

Guenet, B., Eglin, T., Vasilyeva, N., Peylin, P., Ciais, P., and Chenu, C. (2013). The relative importance of decomposition and transport mechanisms in accounting for soil organic carbon profiles. *Biogeosciences*, 10(4):2379–2392.

Guo, L. B. and Gifford, R. M. (2002). Soil carbon stocks and land use change: a meta analysis. *Global Change Biology*, 8(4):345–360.

Guo, X., Mao, X., Yu, W., Xiao, L., Wang, M., Zhang, S., Zheng, J., Zhou, H., Luo, L., Chang, J., Shi, Z., and Luo, Z. (2023). A field incubation approach to evaluate the depth dependence of soil biogeochemical responses to climate change. *Global Change Biology*, 29(3):909–920.

Hansen, S., Jensen, H. E., Nielsen, N. E., and Svendsen, H. (1991). Simulation of nitrogen dynamics and biomass production in winter wheat using the danish simulation model daisy. *Fertilizer research*, 27(2):245–259.

He, Y., Trumbore, S. E., Torn, M. S., Harden, J. W., Vaughn, L. J. S., Allison, S. D., and Randerson, J. T. (2016). Radiocarbon constraints imply reduced carbon uptake by soils during the 21st century. *Science*, 353(6306):1419–1424.

Heckman, K., Hicks Pries, C. E., Lawrence, C. R., Rasmussen, C., Crow, S. E., Hoyt, A. M., von Fromm, S. F., Shi, Z., Stoner, S., McGrath, C., Beem-Miller, J., Berhe, A. A., Blankinship, J. C., Keiluweit, M., Marín-Spiotta, E., Monroe, J. G., Plante, A. F., Schimel, J., Sierra, C. A., Thompson, A., and Wagai, R. (2022). Beyond bulk: Density fractions explain heterogeneity in global soil carbon abundance and persistence. *Global Change Biology*, 28(3):1178–1196.

Hilbert, D. W., Roulet, N., and Moore, T. (2000). Modelling and analysis of peatlands as dynamical systems. *Journal of Ecology*, 88(2):230–242.

Hilinski, T. E. (2001). Implementation of exponential depth distribution of organic carbon in the century model.

Hinzmann, M., Ittner, S., Kiresiewa, Z., and Gerdes, H. (2021). An acceptance analysis of subsoil amelioration amongst agricultural actors in two regions in germany. *Frontiers in Agronomy*, 3.

Hirte, J., Leifeld, J., Abiven, S., Oberholzer, H.-R., and Mayer, J. (2018). Below ground carbon inputs to soil via root biomass and rhizodeposition of field-grown maize and wheat at harvest are independent of net primary productivity. *Agriculture, Ecosystems & Environment*, 265:556–566.

Högberg, P. (1997). Tansley review no. 95 15N natural abundance in soil–plant systems. *The New Phytologist*, 137(2):179–203.

Hole, F. D. (1961). A classification of pedoturbations and some other processes and factors of soil formation in relation to isotropism and anisotropism. *Soil Science*, 91:375–377.

Hoosbeek, M. R. and Scarascia-Mugnozza, G. E. (2009). Increased litter build up and soil organic matter stabilization in a poplar plantation after 6 years of atmospheric co2 enrichment (face): Final results of pop-euroface compared to other forest face experiments. *Ecosystems*, 12(2):220–239.

Huang, Y., Lu, X., Shi, Z., Lawrence, D., Koven, C. D., Xia, J., Du, Z., Kluzek, E., and Luo, Y. (2018). Matrix approach to land carbon cycle modeling: A case study with the community land model. *Global Change Biology*, 24(3):1394–1404.

Jackson, R., Canadell, J., Ehleringer, J., Mooney, H., Sala, O., and Schulze, E. (1996). A global analysis of root distributions for terrestrial biomes. *Oecologia*, 10:389–411.

Jackson, R., Mooney, H., and Schulze, E.-D. (1997). A global budget for fine root biomass, surface area, and nutrient contents. *Proceedings of the National Academy of Sciences USA*, 94:7362–7366.

Jackson, R., Schenk, H., Jobbágy, E., Canadell, J., Colello, G., Dickinson, R., Field, C., Friedlingstein, P., Heimann, M., Hibbard, K., Kicklighter, D., Kleidon, A., Neilson, R., Parton, W., Sala, O., and Sykes, M. (2000). Belowground consequences of vegetation change and their treatment in models. *Ecological Applications*, pages 10(2):470–483.

Jenkinson, D. S. and Coleman, K. (2008). The turnover of organic carbon in subsoils. part 2. modelling carbon turnover. *European Journal of Soil Science*, 59(2):400–413.

Jenny, H. (1980). *The Soil Resource: Origin and Behavior*. Ecological Studies. Springer New York.

Jobbágy, E. and Jackson, R. (2000). The vertical distribution of soil organic carbon and its relation to climate and vegetation. *Ecological Applications*, pages 10(2):423–436.

Johnson, D., Domier, J., and Johnson, D. (2005). Animating the biodynamics of soil thickness using process vector analysis: a dynamic denudation approach to soil formation. *Geomorphology*, 67(1):23–46. Weathering and landscape evolution.

Johnson, D. L., Watson-Stegner, D., Johnson, D. N., and Schaetzl, R. J. (1987). Proisotropic and proanisotropic processes of pedoturbation. *Soil Science*, 143:278–292.

Jordan, C. F. and Escalante, G. (1980). Root productivity in an amazonian rain forest. *Ecology*, 61(1):14–18. 0012-9658 Article type: Full Length Article / Full publication date: Feb., 1980 (198002). / Languages: EN / Copyright 1980 Ecological Society of America.

Kaiser, K. and Kalbitz, K. (2012). Cycling downwards – dissolved organic matter in soils. *Soil Biology and Biochemistry*, 52:29–32.

Kalbitz, K. and Kaiser, K. (2008). Contribution of dissolved organic matter to carbon storage in forest mineral soils. *Journal of Plant Nutrition and Soil Science*, 171(1):52–60.

Kalbitz, K., Solinger, S., Park, J. H., Michalzik, B., and Matzner, E. (2000). Controls on the dynamics of dissolved organic matter in soils: A review. *Soil Science*, 165(4).

Kaste, J. M., Heimsath, A. M., and Bostick, B. C. (2007). Short-term soil mixing quantified with fallout radionuclides. *Geology*, 35(3):243–246.

Kätterer, T., Börjesson, G., and Kirchmann, H. (2014). Changes in organic carbon in topsoil and sub-soil and microbial community composition caused by repeated additions of organic amendments and n fertilisation in a long-term field experiment in sweden. *Agriculture, Ecosystems & Environment*, 189:110–118.

Kautz, T., Amelung, W., Ewert, F., Gaiser, T., Horn, R., Jahn, R., Javaux, M., Kemna, A., Kuzyakov, Y., Munch, J.-C., Pätzold, S., Peth, S., Scherer, H. W., Schloter, M., Schneider, H., Vanderborght, J., Vetterlein, D., Walter, A., Wiesenberg, G. L., and Köpke, U. (2013). Nutrient acquisition from arable subsoils in temperate climates: A review. *Soil Biology and Biochemistry*, 57:1003–1022.

Kell, D. B. (2011). Breeding crop plants with deep roots: their role in sustainable carbon, nutrient and water sequestration. *Annals of Botany*, 108(3):407–418.

Kindler, R., SIEMENS, J., KAISER, K., WALMSLEY, D. C., BERNHOFER, C., BUCHMANN, N., CELLIER, P., EUGSTER, W., GLEIXNER, G., GRÜNWALD, T., HEIM, A., IBROM, A., JONES, S. K., JONES, M., KLUMPP, K., KUTSCH, W., LARSEN, K. S., LEHUGER, S., LOUBET, B., MCKENZIE, R., MOORS, E., OSBORNE, B., PILEGAARD, K., REBMANN, C., SAUNDERS, M., SCHMIDT, M. W. I., SCHRUMPF, M., SEYFFERTH, J., SKIBA, U., SOUSSANA, J.-F., SUTTON, M. A., TEFS, C., VOWINCKEL, B., ZEEMAN, M. J., and KAUPENJOHANN, M. (2011). Dissolved carbon leaching from soil is a crucial component of the net ecosystem carbon balance. *Global Change Biology*, 17(2):1167–1185.

Kirchmann, H., Schön, M., Börjesson, G., Hamnér, K., and Kätterer, T. (2013). Properties of soils in the swedish long-term fertility experiments: Vii. changes in topsoil and upper subsoil at örja and fors after 50 years of nitrogen fertilization and manure application. *Acta Agriculturae Scandinavica, Section B — Soil & Plant Science*, 63(1):25–36.

Kirkby, M. J. (1977). Soil development models as a component of slope models. *Earth Surface Processes*, 2(2-3):203–230.

Koven, C., Friedlingstein, P., Ciais, P., Khvorostyanov, D., Krinner, G., and Tarnocai, C. (2009). On the formation of high-latitude soil carbon stocks: Effects of cryoturbation and insulation by organic matter in a land surface model. *Geophysical Research Letters*, 36(21).

Koven, C. D., Riley, W. J., Subin, Z. M., Tang, J. Y., Torn, M. S., Collins, W. D., Bonan, G. B., Lawrence, D. M., and Swenson, S. C. (2013). The effect of vertically resolved soil biogeochemistry and alternate soil c and n models on c dynamics of clm4. *Biogeosciences*, 10(11):7109–7131.

Lanczos, C. (1996). *Linear Differential Operators*. Society for Industrial and Applied Mathematics.

Lawrence, C. R., Beem-Miller, J., Hoyt, A. M., Monroe, G., Sierra, C. A., Stoner, S., Heckman, K., Blankinship, J. C., Crow, S. E., McNicol, G., Trumbore, S., Levine, P. A., Vindušková, O., Todd-Brown, K., Rasmussen, C., Hicks Pries, C. E., Schädel, C., McFarlane, K., Doetterl, S., Hatté, C., He, Y., Treat, C., Harden, J. W., Torn, M. S., Estop-Aragonés, C., Asefaw Berhe, A., Keiluweit, M., Della Rosa Kuhnen, A., Marin-Spiotta, E., Plante, A. F., Thompson, A., Shi, Z., Schimel, J. P., Vaughn, L. J. S., von Fromm, S. F., and Wagai, R. (2020). An open-source database for the synthesis of soil radiocarbon data: International Soil Radiocarbon Database (ISRaD) version 1.0. *Earth System Science Data*, 12(1):61–76.

LeVeque, R. J. (1990). *Numerical Methods for Conservation Laws*. Birkhäuser Basel.

LeVeque, R. J. (2007). *Finite difference methods for ordinary and partial differential equations: steady-state and time-dependent problems*. Society for Industrial and Applied Mathematics, Philadelphia, PA. 2007061732 Randall J. LeVeque. ill. ; 26 cm. Includes bibliographical references (p. 329-335) and index.

Li, C., Frolking, S., and Frolking, T. A. (1992). A model of nitrous oxide evolution from soil driven by rainfall events: 1. model structure and sensitivity. *Journal of Geophysical Research: Atmospheres*, 97(D9):9759–9776.

Liang, J., Zhou, Z., Huo, C., Shi, Z., Cole, J. R., Huang, L., Konstantinidis, K. T., Li, X., Liu, B., Luo, Z., Penton, C. R., Schuur, E. A. G., Tiedje, J. M., Wang, Y.-P., Wu, L., Xia, J., Zhou, J., and Luo, Y. (2018). More replenishment than priming loss of soil organic carbon with additional carbon input. *Nature Communications*, 9(1):3175.

Lorenz, K. and Lal, R. (2005). The depth distribution of soil organic carbon in relation to land use and management and the potential of carbon sequestration in subsoil horizons. *Advances in Agronomy*, 88:35–66.

Lu, X., Wang, Y.-P., Luo, Y., and Jiang, L. (2018). Ecosystem carbon transit versus turnover times in response to climate warming and rising atmospheric CO_2 concentration. *Biogeosciences*, 15(21):6559–6572.

Luo, Z., Luo, Y., Wang, G., Xia, J., and Peng, C. (2020). Warming-induced global soil carbon loss attenuated by downward carbon movement. *Global Change Biology*, 26(12):7242–7254.

Manzoni, S., Katul, G. G., and Porporato, A. (2009). Analysis of soil carbon transit times and age distributions using network theories. *J. Geophys. Res.*, 114.

Manzoni, S. and Porporato, A. (2009). Soil carbon and nitrogen mineralization: Theory and models across scales. *Soil Biology and Biochemistry*, 41(7):1355 – 1379.

Marin-Spiotta, E., Chadwick, O. A., Kramer, M., and Carbone, M. S. (2011). Carbon delivery to deep mineral horizons in hawaiian rain forest soils. *Journal of Geophysical Research: Biogeosciences*, 116(G3).

Mathieu, J. A., Hatté, C., Balesdent, J., and Parent, É. (2015). Deep soil carbon dynamics are driven more by soil type than by climate: a worldwide meta-analysis of radiocarbon profiles. *Global Change Biology*, 21(11):4278–4292.

Menichetti, L., Ekblad, A., and Kätterer, T. (2015). Contribution of roots and amendments to soil carbon accumulation within the soil profile in a long-term field experiment in sweden. *Agriculture, Ecosystems & Environment*, 200:79–87.

Metzler, H. and Sierra, C. A. (2018). Linear autonomous compartmental models as continuous-time Markov chains: Transit-time and age distributions. *Mathematical Geosciences*, 50(1):1–34.

Metzler, H., Zhu, Q., Riley, W., Hoyt, A., Müller, M., and Sierra, C. A. (2020). Mathematical reconstruction of land carbon models from their numerical output: Computing soil radiocarbon from c dynamics. *Journal of Advances in Modeling Earth Systems*, 12(1):e2019MS001776. e2019MS001776 10.1029/2019MS001776.

Meysman, F. J., Boudreau, B. P., and Middelburg, J. J. (2005). Modeling reactive transport in sediments subject to bioturbation and compaction. *Geochimica et Cosmochimica Acta*, 69(14):3601–3617.

Meysman, F. J., Malyuga, V. S., Boudreau, B. P., and Middelburg, J. J. (2008). A generalized stochastic approach to particle dispersal in soils and sediments. *Geochimica et Cosmochimica Acta*, 72(14):3460–3478.

Meysman, F. J., Middelburg, J. J., and Heip, C. H. (2006). Bioturbation: a fresh look at darwin's last idea. *Trends in Ecology & Evolution*, 21(12):688–695.

Meysman, F. J. R., Boudreau, B. P., and Middelburg, J. J. (2003). Relations between local, nonlocal, discrete and continuous models of bioturbation. *Journal of Marine Research*, 61:391–410.

Meysman, F. J. R., Boudreau, B. P., and Middelburg, J. J. (2010). When and why does bioturbation lead to diffusive mixing. *Journal of Marine Research*, 68:881–920.

Michalzik, B., Kalbitz, K., Park, J. H., Solinger, S., and Matzner, E. (2001). Fluxes and concentrations of dissolved organic carbon and nitrogen –a synthesis for temperate forests. *Biogeochemistry*, 52(2):173–205.

Michalzik, B., Tipping, E., Mulder, J., Lancho, J. F. G., Matzner, E., Bryant, C. L., Clarke, N., Lofts, S., and Esteban, M. A. V. (2003). Modelling the production and transport of dissolved organic carbon in forest soils. *Biogeochemistry*, 66(3):241–264.

Moni, C., Rumpel, C., Virto, I., Chabbi, A., and Chenu, C. (2010). Relative importance of sorption versus aggregation for organic matter storage in subsoil horizons of two contrasting soils. *European Journal of Soil Science*, 61(6):958–969.

Morari, F., Berti, A., Dal Ferro, N., and Piccoli, I. (2019). *Deep Carbon Sequestration in Cropping Systems*, pages 33–65. Springer International Publishing, Cham.

Moyano, F. E., Manzoni, S., and Chenu, C. (2013). Responses of soil heterotrophic respiration to moisture availability: An exploration of processes and models. *Soil Biology and Biochemistry*, 59(0):72 – 85.

Müller-Lemans, H. and van Dorp, F. (1996). Bioturbation as a mechanism for radionuclide transport in soil: Relevance of earthworms. *Journal of Environmental Radioactivity*, 31(1):7–20.

Nadelhoffer, K. J. and Fry, B. (1988). Controls on natural nitrogen-15 and carbon-13 abundances in forest soil organic matter. *Soil Science Society of America Journal*, 52(6):1633–1640.

Nakane, K. and Shinozaki, K. (1978). A mathematical model of the behavior and vertical distribution of organic carbon in forest soils. *JAPANESE JOURNAL OF ECOLOGY*, 28(2):111–122.

Neff, J. C. and Asner, G. P. (2001). Dissolved organic carbon in terrestrial ecosystems: Synthesis and a model. *Ecosystems*, 4(1):29–48.

Nguyen, C. (2009). *Rhizodeposition of Organic C by Plant: Mechanisms and Controls*, pages 97–123. Springer Netherlands, Dordrecht.

O'Brien, B. and Stout, J. (1978). Movement and turnover of soil organic matter as indicated by carbon isotope measurements. *Soil Biology and Biochemistry*, 10(4):309 – 317.

Paton, T., Humphreys, G., and Mitchell, P. (1995). *Soils: A New Global View*. Yale University Press.

Paul, A., Balesdent, J., and Hatté, C. (2020). 13c-14c relations reveal that soil 13c-depth gradient is linked to historical changes in vegetation 13c. *Plant and Soil*, 447(1):305–317.

Pausch, J. and Kuzyakov, Y. (2018). Carbon input by roots into the soil: Quantification of rhizodeposition from root to ecosystem scale. *Global Change Biology*, 24(1):1–12.

Persson, T., Karlsson, P. S., Seyferth, U., Sjöberg, R. M., and Rudebeck, A. (2000). *Carbon Mineralisation in European Forest Soils*, pages 257–275. Springer Berlin Heidelberg, Berlin, Heidelberg.

Poeplau, C. and Don, A. (2013). Sensitivity of soil organic carbon stocks and fractions to different land-use changes across europe. *Geoderma*, 192:189–201.

Ponce-Hernandez, R., Marriott, F. H. C., and Beckett, P. H. T. (1986). An improved method for reconstructing a soil profile from analyses of a small number of samples. *Journal of Soil Science*, 37(3):455–467.

Raich, J. and Nadelhoffer, K. (1989). Belowground carbon allocation in forest ecosystems: global trends. *Ecology*, 70(5):1346–1354.

1084 Rasmussen, C., Heckman, K., Wieder, W. R., Keiluweit, M., Lawrence, C. R., Berhe, A. A., Blank-
1085   inship, J. C., Crow, S. E., Druhan, J. L., Hicks Pries, C. E., Marin-Spiotta, E., Plante, A. F.,
1086   Schädel, C., Schimel, J. P., Sierra, C. A., Thompson, A., and Wagai, R. (2018). Beyond clay:
1087   towards an improved set of variables for predicting soil organic matter content. *Biogeochemistry*,
1088   137(3):297–306.

1089 Rasse, D. P., Rumpel, C., and Dignac, M.-F. (2005). Is soil carbon mostly root carbon? mechanisms
1090   for a specific stabilisation. *Plant and Soil*, 269(1):341–356.

1091 Rosenbloom, N. A., Doney, S. C., and Schimel, D. S. (2001). Geomorphic evolution of soil texture
1092   and organic matter in eroding landscapes. *Global Biogeochemical Cycles*, 15(2):365–381.

1093 Roth, V.-N., Lange, M., Simon, C., Hertkorn, N., Bucher, S., Goodall, T., Griffiths, R. I., Mellado-
1094   Vázquez, P. G., Mommer, L., Oram, N. J., Weigelt, A., Dittmar, T., and Gleixner, G. (2019).
1095   Persistence of dissolved organic matter explained by molecular changes during its passage through
1096   soil. *Nature Geoscience*, 12(9):755–761.

1097 Rumpel, C., Chabbi, A., and Marschner, B. (2012). *Carbon Storage and Sequestration in Subsoil
1098   Horizons: Knowledge, Gaps and Potentials*, pages 445–464. Springer Netherlands, Dordrecht.

1099 Rumpel, C. and Kögel-Knabner, I. (2011). Deep soil organic matter—a key but poorly understood
1100   component of terrestrial c cycle. *Plant and Soil*, 338(1):143–158.

1101 Rumpel, C., Kögel-Knabner, I., and Bruhn, F. (2002). Vertical distribution, age, and chemical
1102   composition of organic carbon in two forest soils of different pedogenesis. *Organic Geochemistry*,
1103   33(10):1131–1142.

1104 Salvador-Blanes, S., Minasny, B., and McBratney, A. B. (2007). Modelling long-term in situ soil profile
1105   evolution: application to the genesis of soil profiles containing stone layers. *European Journal of
1106   Soil Science*, 58(6):1535–1548.

1107 Sanderman, J., Baldock, J. A., and Amundson, R. (2008). Dissolved organic carbon chemistry and
1108   dynamics in contrasting forest and grassland soils. *Biogeochemistry*, 89(2):181–198.

1109 Sarmiento, J. and Gruber, N. (2006). *Ocean Biogeochemical Dynamics*. Princeton University Press,
1110   Princeton.

1111 Saugier, B., Roy, J., and Mooney, H. (2001). Estimations of global terrestrial productivity: Converg-
1112   ing toward a single number? In Roy, J., Saugier, and B Mooney, H., editors, *Terrestrial Global
1113   Productivity*. Academic Press.

1114 Scheibe, A., Sierra, C. A., and Spohn, M. (2023). Recently fixed carbon fuels microbial activity several
1115   meters below the soil surface. *Biogeosciences*, 20(4):827–838.

1116 Schenk, H. and Jackson, R. (2002a). The global biogeography of roots. *Ecological Monographs*, pages
1117   72(3):311–328.

1118 Schenk, H. and Jackson, R. (2002b). Rooting depths, lateral root spreads and below-ground/above-
1119   ground allometries of plants in water limited ecosystem. *Journal of Ecology*, pages 90:480–494.

1120 Schimel, J. P. and Weintraub, M. N. (2003). The implications of exoenzyme activity on micro-
1121   bial carbon and nitrogen limitation in soil: a theoretical model. *Soil Biology and Biochemistry*,
1122   35(4):549–563.

1123 Shi, Z., Allison, S. D., He, Y., Levine, P. A., Hoyt, A. M., Beem-Miller, J., Zhu, Q., Wieder, W. R.,
1124   Trumbore, S., and Randerson, J. T. (2020). The age distribution of global soil carbon inferred from
1125   radiocarbon measurements. *Nature Geoscience*, 13(8):555–559.

Sierra, C. A., Ceballos-Núñez, V., Metzler, H., and Müller, M. (2018a). Representing and understanding the carbon cycle using the theory of compartmental dynamical systems. *Journal of Advances in Modeling Earth Systems*, 10(8):1729–1734.

Sierra, C. A., Crow, S. E., Heimann, M., Metzler, H., and Schulze, E.-D. (2021a). The climate benefit of carbon sequestration. *Biogeosciences*, 18(3):1029–1048.

Sierra, C. A., Estupinan-Suarez, L. M., and Chanca, I. (2021b). The fate and transit time of carbon in a tropical forest. *Journal of Ecology*, 109(8):2845–2855.

Sierra, C. A., Hoyt, A. M., He, Y., and Trumbore, S. E. (2018b). Soil organic matter persistence as a stochastic process: Age and transit time distributions of carbon in soils. *Global Biogeochemical Cycles*, 32(10):1574–1588.

Sierra, C. A. and Müller, M. (2015). A general mathematical framework for representing soil organic matter dynamics. *Ecological Monographs*, 85:505–524.

Sierra, C. A., Müller, M., Metzler, H., Manzoni, S., and Trumbore, S. E. (2017). The muddle of ages, turnover, transit, and residence times in the carbon cycle. *Global Change Biology*, 23(5):1763–1773.

Sierra, C. A., Trumbore, S. E., Davidson, E. A., Vicca, S., and Janssens, I. (2015). Sensitivity of decomposition rates of soil organic matter with respect to simultaneous changes in temperature and moisture. *Journal of Advances in Modeling Earth Systems*, 7(1):335–356.

Slessarev, E. W., Nuccio, E. E., McFarlane, K. J., Ramon, C. E., Saha, M., Firestone, M. K., and Pett-Ridge, J. (2020). Quantifying the effects of switchgrass (panicum virgatum) on deep organic c stocks using natural abundance 14c in three marginal soils. *GCB Bioenergy*, 12(10):834–847.

Thompson, M. V. and Randerson, J. T. (1999). Impulse response functions of terrestrial carbon cycle models: method and application. *Global Change Biology*, 5(4):371–394. 10.1046/j.1365-2486.1999.00235.x.

Thorup-Kristensen, K., Halberg, N., Nicolaisen, M., Olesen, J. E., Crews, T. E., Hinsinger, P., Kirkegaard, J., Pierret, A., and Dresbøll, D. B. (2020). Digging deeper for agricultural resources, the value of deep rooting. *Trends in Plant Science*, 25(4):406–417.

Tonneijck, F. H. and Jongmans, A. G. (2008). The influence of bioturbation on the vertical distribution of soil organic matter in volcanic ash soils: a case study in northern ecuador. *European Journal of Soil Science*, 59(6):1063–1075.

van Breemen, N. and Buurman, P. (1997). *Soil Formation*. Kluwer Academic Publishers.

van Dam, D., van Breemen, N., and Veldkamp, E. (1997). Soil organic carbon dynamics: variability with depth in forested and deforested soils under pasture in costa rica. *Biogeochemistry*, 39(3):343–375.

van Veen, J. A. and Paul, E. A. (1981). Organic carbon dynamics in grassland soils. 1. background information and computer simulation. *Canadian Journal of Soil Science*, 61(2):185–201.

Vancampenhout, K., De Vos, B., Wouters, K., Swennen, R., Buurman, P., and Deckers, J. (2012). Organic matter of subsoil horizons under broadleaved forest: Highly processed or labile and plant-derived? *Soil Biology and Biochemistry*, 50:40–46.

VandenBygaart, A. J., Bremer, E., McConkey, B. G., Ellert, B. H., Janzen, H. H., Angers, D. A., Carter, M. R., Drury, C. F., Lafond, G. P., and McKenzie, R. H. (2011). Impact of sampling depth on differences in soil carbon stocks in long-term agroecosystem experiments. *Soil Science Society of America Journal*, 75(1):226–234.

Wang, G., Xiao, L., Lin, Z., Zhang, Q., Guo, X., Cowie, A., Zhang, S., Wang, M., Chen, S., Zhang, G., Shi, Z., Sun, W., and Luo, Z. (2023). Most root-derived carbon inputs do not contribute to long-term global soil carbon storage. *Science China Earth Sciences*, 66(5):1072–1086.

Xiao, L., Wang, G., Chang, J., Chen, Y., Guo, X., Mao, X., Wang, M., Zhang, S., Shi, Z., Luo, Y., Cheng, L., Yu, K., Mo, F., and Luo, Z. (2023). Global depth distribution of belowground net primary productivity and its drivers. *Global Ecology and Biogeography*, in press.

Xiao, L., Wang, G., Wang, M., Zhang, S., Sierra, C. A., Guo, X., Chang, J., Shi, Z., and Luo, Z. (2022). Younger carbon dominates global soil carbon efflux. *Global Change Biology*, 28(18):5587–5599.

Yoo, K., Ji, J., Aufdenkampe, A., and Klaminder, J. (2011). Rates of soil mixing and associated carbon fluxes in a forest versus tilled agricultural field: Implications for modeling the soil carbon cycle. *Journal of Geophysical Research: Biogeosciences*, 116(G1).
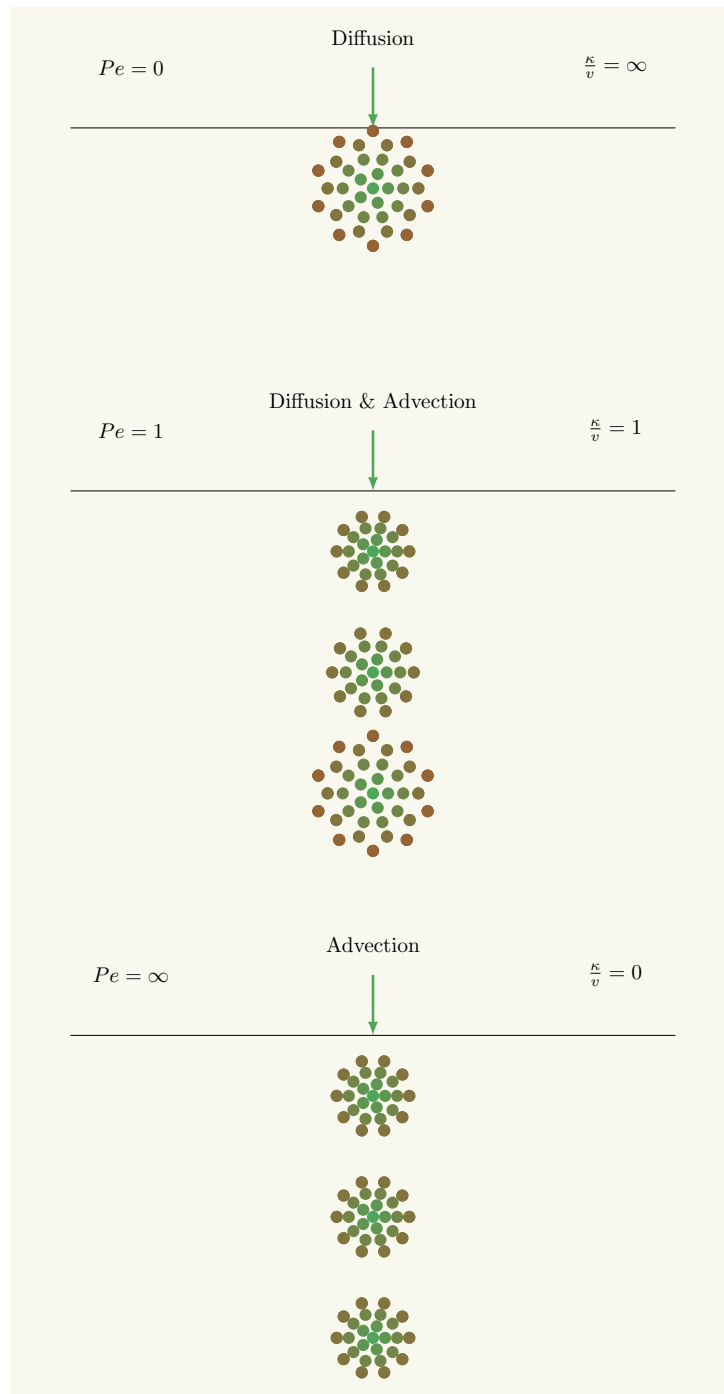
Figure 1: Schematic representation of the role of the Péclet number, which is the inverse of the κ/v ratio, on the type of vertical C transfer in a soil assuming a pulse of aboveground inputs. For a Péclet number of zero and $\kappa/v = \infty$, C entering the soil only moves due to diffusion (top); for a Péclet number and $\kappa/v = 1$, both diffusion and advection moves the carbon vertically (center); for a Péclet number of ∞ and $\kappa/v = 0$, C is only moved vertically by advective processes as in the case of DOC transport (bottom).
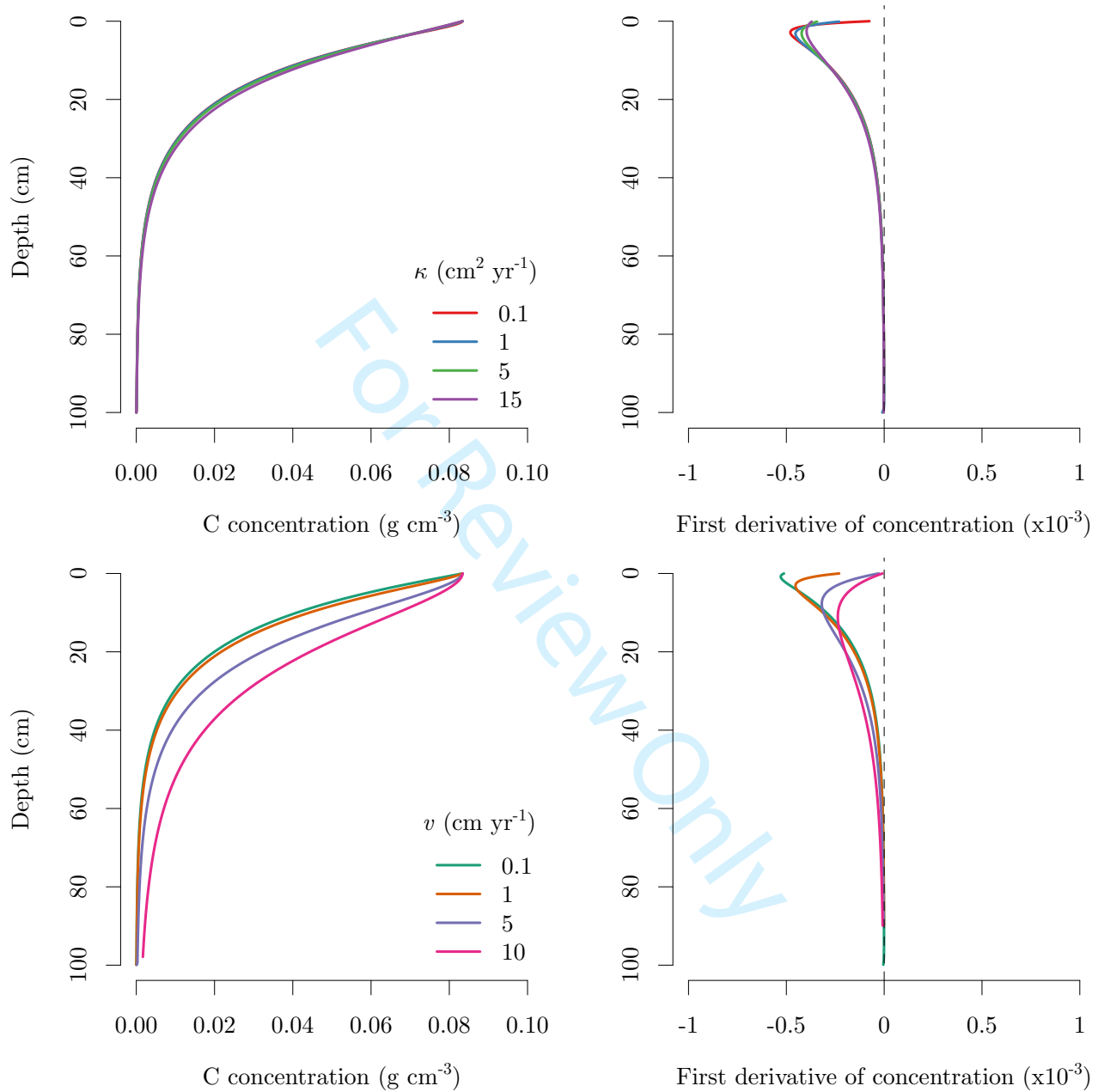
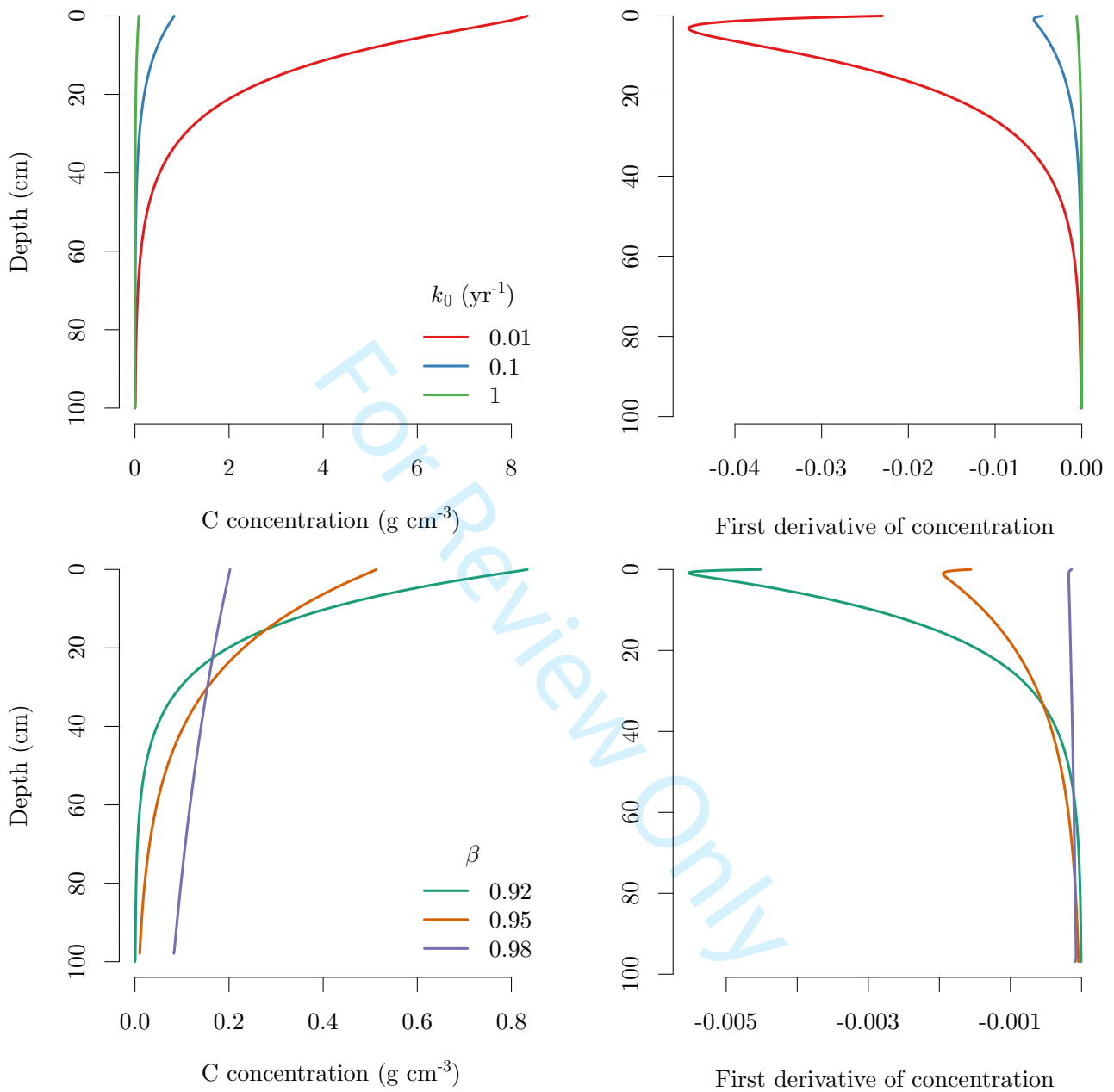Figure 2: Numerical simulations of soil C depth profiles using the linear model with constant coefficients of equation 17. The top panels show the C concentration and the first derivative of C concentrations for different values of κ and a fixed value of $v = 1$ cm yr^{-1}. The bottom panels show C concentrations and their first derivative for different values of v and a constant value of $\kappa = 1$ cm^2 yr^{-1}.

Figure 3: Numerical simulations of soil C depth profiles using the linear model with constant coefficients of equation 17. The top panels show C concentration and its first derivative with respect to depth for different functions representing decomposition rate $k(d)$ (equation 19). The different lines are the results of the model for different values of the maximum decomposition rate at the surface k_0, with the value of $k_0 = 1$ yr^{-1} representing fast decomposition and $k_0 = 0.01$ yr^{-1} slow decomposition. The lower panels represent the results of simulation for different shapes of the root input profile according to equation 18, with the parameter $\beta = 0.98$ representing deep root inputs, and $\beta = 0.92$ shallow root inputs.
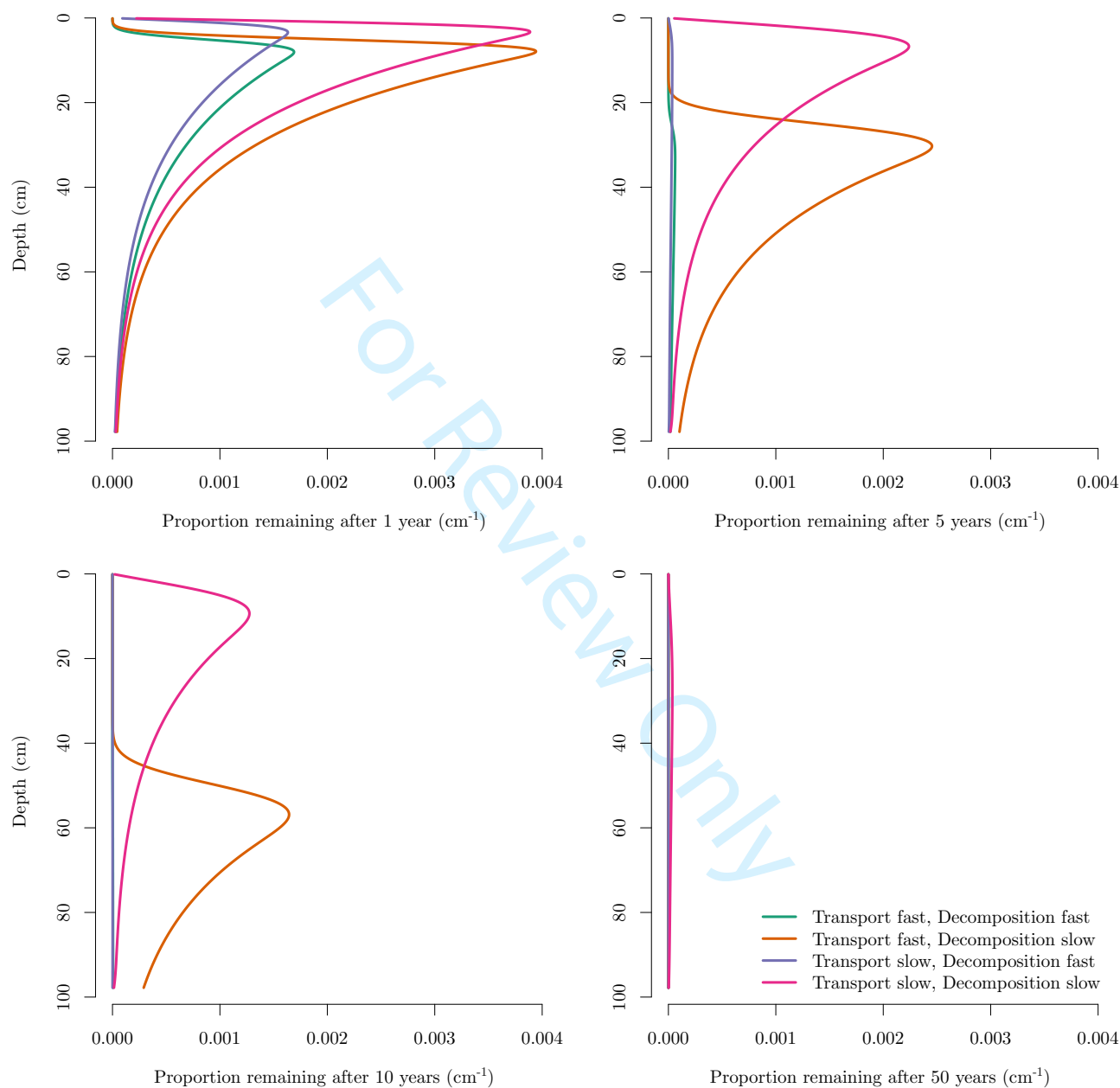
Figure 4: Proportion of C remaining in a soil profile of an amount of lateral inputs entering the soil at $t = 0$ represented with equation 18 with $\beta = 0.95$. After 50 years most of the carbon that entered at $t = 0$ is not present in the soil, even for the scenario with slow transport and decomposition rates.
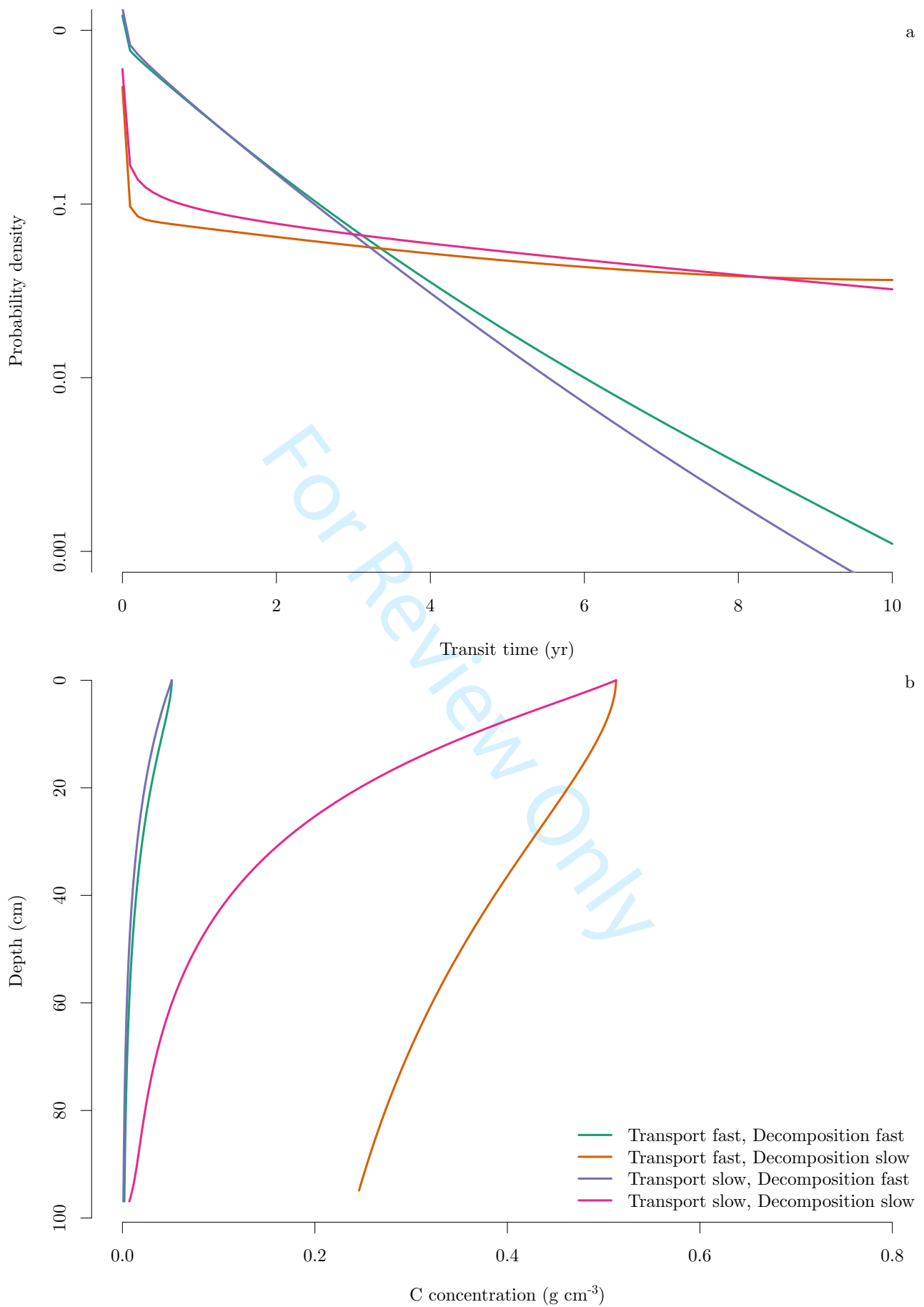
Figure 5: (a) Transit time distributions for four different scenarios of transport and decomposition in the subsoil. These distributions represent the proportion of C leaving the soil system at different times since the C entered the soil. Note the logarithmic y axis. (b) Values of C concentration along the depth profile at steady-state.
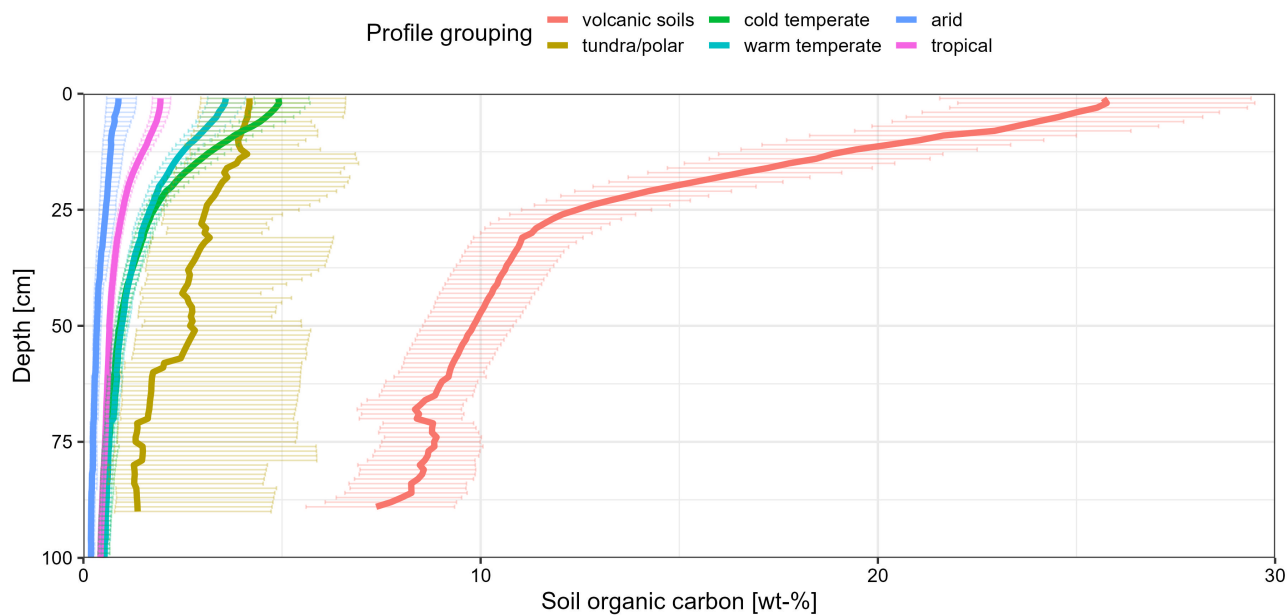
Figure 6: Soil carbon concentrations at different depths from the International Soil Radiocarbon Database, with data from 600 profiles aggregated by biogeographical regions. Thick lines for each group represent the mean across available observations and fitted to a spline curve. Horizontal lines represent standard deviation across available observations.
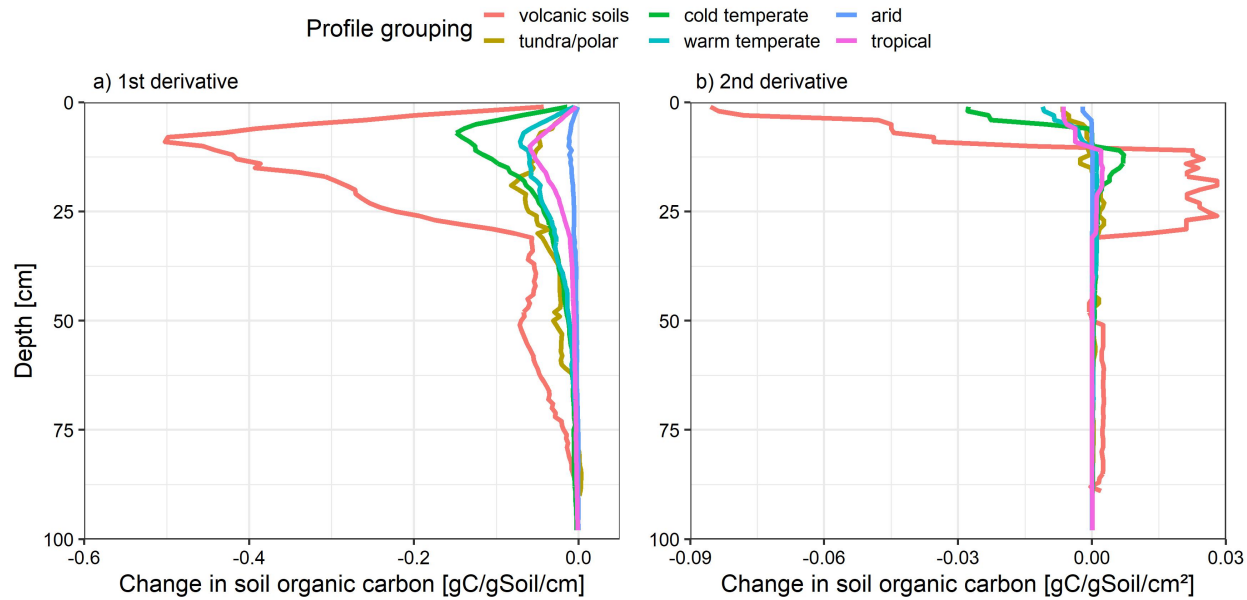

Figure 7: First and second derivative of soil C profiles extracted from ISRaD and grouped by biogeographical region, with the exception of volcanic soils.
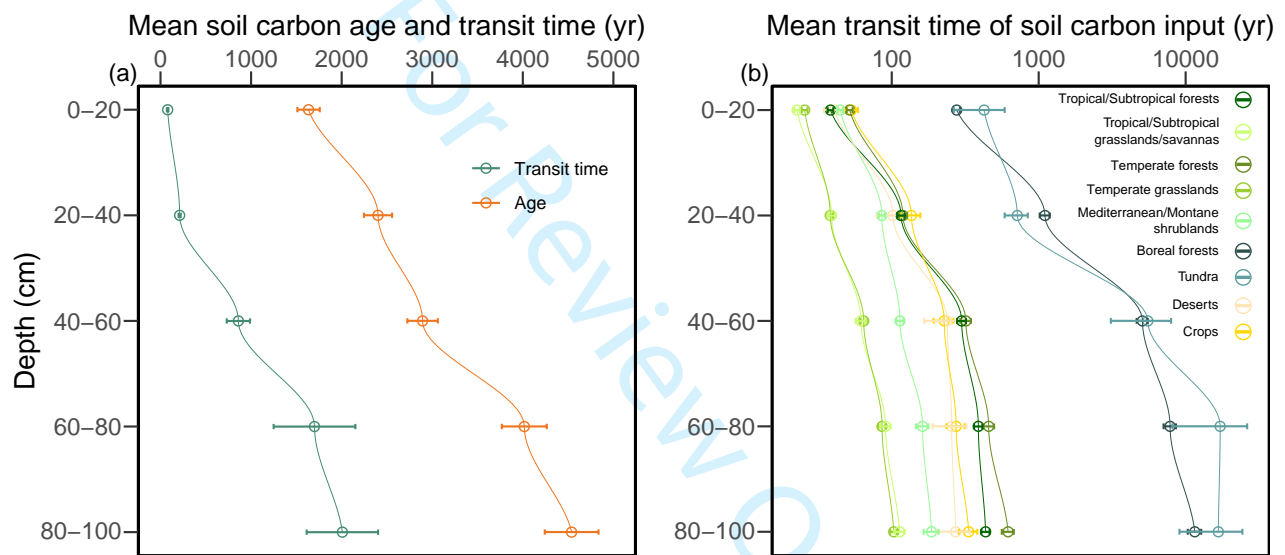
Figure 8: Estimates of mean age and mean transit time of carbon based on measurements of root inputs and soil radiocarbon obtained from ISRaD. The left panel shows global-scale average values of mean age and mean transit time. The right panel shows averages of mean transit time averaged by biome.